



Math-PUMA: Progressive Upward Multimodal Alignment to Enhance Mathematical Reasoning

Wenwen Zhuang^{1*}, Xin Huang^{2*}, Xiantao Zhang^{3*}, Jin Zeng¹

¹University of Chinese Academy of Sciences

²Beijing Institute of Technology ³Beihang University

zhuangwenwen23@mails.ucas.ac.cn, huangxin@bit.edu.cn, zhangxiantao@buaa.edu.cn

Abstract

Multimodal Large Language Models (MLLMs) excel in solving text-based mathematical problems, but they struggle with mathematical diagrams since they are primarily trained on natural scene images. For humans, visual aids generally enhance problem-solving, but MLLMs perform worse as information shifts from textual to visual modality. This decline is mainly due to their shortcomings in aligning images and text. To tackle aforementioned challenges, we propose Math-PUMA, a methodology focused on **Progressive Upward Multimodal Alignment**. This approach is designed to improve the mathematical reasoning skills of MLLMs through a three-stage training process, with the second stage being the critical alignment stage. We first enhance the language model’s mathematical reasoning capabilities with extensive set of textual mathematical problems. We then construct a multimodal dataset with varying degrees of textual and visual information, creating data pairs by presenting each problem in at least two forms. By leveraging the Kullback-Leibler (KL) divergence of next-token prediction distributions to align visual and textual modalities, consistent problem-solving abilities are ensured. Finally, we utilize multimodal instruction tuning for MLLMs with high-quality multimodal data. Experimental results on multiple mathematical reasoning benchmarks demonstrate that the MLLMs trained with Math-PUMA surpass most open-source MLLMs. Our approach effectively narrows the performance gap for problems presented in different modalities. The code and data are available at: <https://github.com/wwzhuang01/Math-PUMA>.

Introduction

Large Language Models (LLMs) have demonstrated remarkable reasoning capabilities, particularly when tackling mathematical problems in textual form (Wei et al. 2022; Chen et al. 2022; Gou et al. 2023; Yu et al. 2023; Shao et al. 2024). However, Multimodal Large Language Models (MLLMs) face greater challenges when tackling problems that involve images. These models need to not only interpret textual information but also comprehend mathematical diagrams and identify details crucial for solving problems. Although MLLMs have exhibited notable efficacy in general visual question answering (Radford et al. 2021; Li et al. 2022; Liu et al. 2023), their training predominantly relies on

*These authors contributed equally.

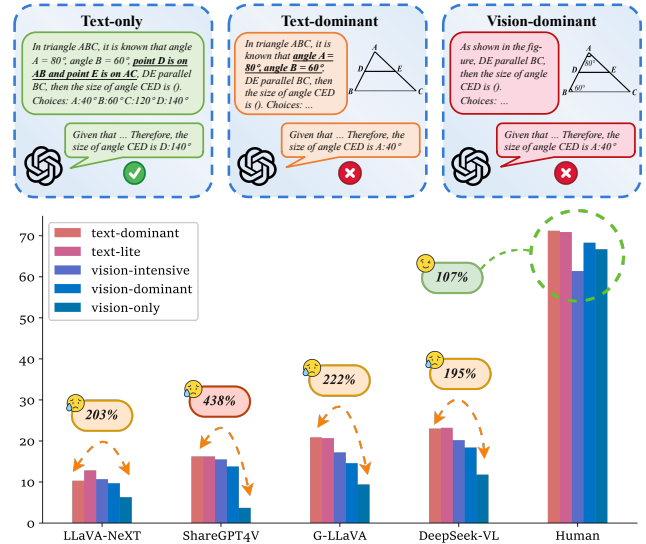


Figure 1: (Top) Three examples of GPT-4o solving multimodal math problems. These examples represent different modalities of the same question. (Bottom) Results of several open-source MLLMs and human on five different tasks of MATHVERSE (Zhang et al. 2024).

datasets comprising natural scene images. This reliance engenders a substantial domain discrepancy when these models are applied to mathematical diagrams, thereby resulting in inferior performance.

For humans, regardless of the modality in which information is presented, problems with equivalent amounts of information tend to have similar levels of difficulty. Furthermore, incorporating images into problem-solving tasks can enhance human comprehension and resolution abilities. As illustrated in Figure 1, an increase in visual data often correlates with a decline in the efficacy of most MLLMs. Additionally, there is a notable disparity in effectiveness between text-centric and exclusively visual problems. For example, GPT-4o (OpenAI 2024b) demonstrates strong proficiency in solving text-only mathematical problems, but its effectiveness diminishes progressively as the modality transitions from textual to visual. This reduction in capability primarily stems from the current models’ inadequate align-

ment between visual and textual data, which impairs their overall functionality.

To address this issue, we propose Math-PUMA, a methodology centered around **Progressive Upward Multimodal Alignment (PUMA)**, aimed at enhancing the mathematical reasoning capabilities of MLLMs. Our approach is structured into three distinct stages, with stage 2 serving as the pivotal alignment phase. **(1) Stage 1:** We train the LLM using a substantial dataset of text-based math problems to enhance its problem-solving capabilities. This phase capitalizes on the extensive availability of text-based math problem-solving data. **(2) Stage 2:** It is observed that the model’s mathematical problem-solving ability diminished progressively from text to vision, exhibiting an upward pyramidal structure. Consequently, the model’s capabilities are categorized into four hierarchical levels. We construct 692K data pairs, with each pair conveying identical information but differing in multimodal representation. By leveraging the KL-divergence between next-token prediction distributions for text-rich and vision-rich problems, we achieve progressive bottom-up modal alignment across these hierarchical levels, thereby enhancing the model’s ability to tackle multimodal mathematical problems. **(3) Stage 3:** We select 996K high-quality multimodal problem-solving data to fine-tune the model, further enhancing its performance in multimodal mathematical problem-solving tasks.

The contributions of this paper are three-fold:

- We curate a large-scale dataset, Math-PUMA-1M, which comprises 692K data pairs and 996K multimodal mathematical data. This dataset serves as a valuable resource for model training.
- We propose Math-PUMA, a methodology based on Progressive Upward Multimodal Alignment, which enhances mathematical reasoning in MLLMs through a three-stage process.
- Experimental results on three widely-used benchmarks demonstrate that the MLLMs trained with Math-PUMA outperform most open-source models. Notably, our approach effectively narrows the performance gap for problems that contain the same information but are presented in different modalities, as evidenced by results on MATH-VERSE.

Related Work

Multimodal Large Language Models

The exploration of Multimodal Large Language Models (MLLMs) has been inspired by advancements in Large Language Models (LLMs), resulting in remarkable capabilities across a variety of tasks that require both visual and linguistic understanding. CLIP (Radford et al. 2021) is a breakthrough model that learns transferable visual representations from natural language supervision. LLaVA series (Liu et al. 2023, 2024a) pioneer visual instruction tuning for LLMs, employing a simple MLP as a projector to connect the vision encoder with the language model. Models such as Qwen-VL (Bai et al. 2023) and Deepseek-VL (Lu et al. 2024a) introduce a new visual receptor or a hybrid vision

encoder, significantly enhancing their ability to perceive and understand visual inputs. However, despite these significant strides, MLLMs still face considerable challenges, particularly in multimodal mathematical reasoning. This is primarily due to the substantial domain gap between the natural scene image and the abstract mathematical graphics. There is a pressing need to enhance the understanding and reasoning abilities of MLLMs in relation to mathematical diagrams.

Multimodal Mathematical Reasoning

The advancement of MLLMs has driven significant research into multimodal reasoning. Current efforts are primarily centered on data augmentation to improve models’ performance. Significant efforts have been invested in augmenting text-only mathematical problem-solving data to enhance LLMs’ reasoning capabilities (Saxton et al. 2019; Yu et al. 2023; Liu and Yao 2024). G-LLaVA (Gao et al. 2023a) and Math-LLaVA (Shi et al. 2024) improve multimodal mathematical reasoning by constructing the Geo170K and MathV360K datasets, respectively. These are created by generating additional questions for images sourced from public datasets. However, they only serve to expand the text, without increasing the diversity of images in the dataset. GeoGPT4V (Cai et al. 2024) leverages GPT-4V (OpenAI 2023b) to generate new problems and images based on existing datasets, creating a dataset of 4.9K geometric problems combined with 19K open-source data. Nevertheless, due to GPT-4V’s subpar capability in generating code from image descriptions, the quality of the generated data is comparatively inferior. By comparison, our work not only makes new advancements in data augmentation, including text rephrasing and the generation of high-quality images, but also introduces a novel alignment method used for training.

Methodology

Data Construction

In order to refine alignment between visual and textual modalities, we need to construct data pairs. We clarify a **“data pair”** as a set of two data components, which share an equivalent level of information within each problem context, and their solutions are identical. A **“data pair”** is defined as two data components that contain equivalent information within the same problem context, and their solutions are identical. However, the distribution of information across different modalities may vary within each pair. We use the term **“vision-rich”** to describe the data component where the visual modality has a higher proportion of information, whereas **“text-rich”** refers to the component with a higher proportion of textual information.

The methods we employ to construct data pairs include automatic data generation and data augmentation based on publicly available sources.

Automatic Data Generation We implement an automatic data generation pipeline for three categories of mathematical problems: plane geometry, solid geometry, and functions. The pipeline consists of four agents: **(1) Question**

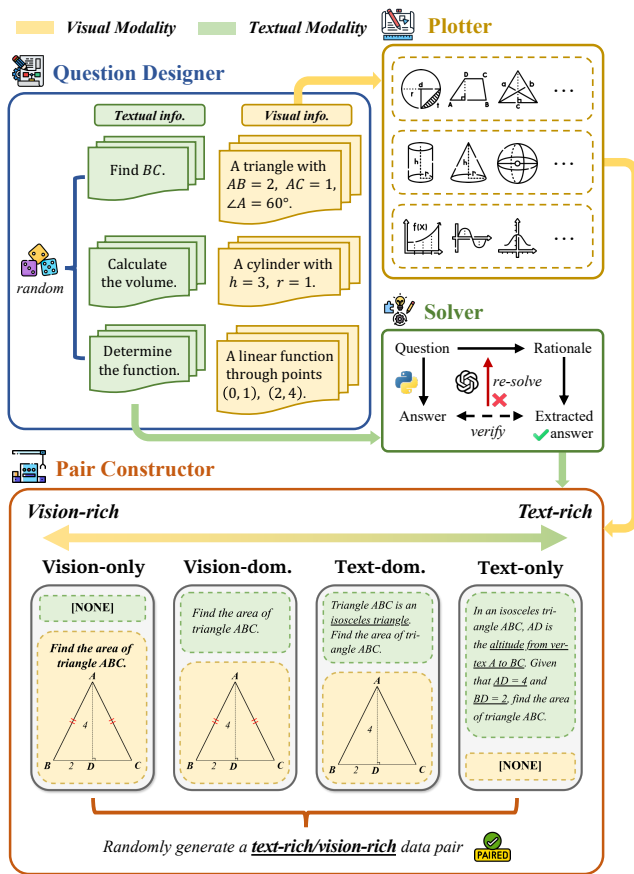


Figure 2: The pipeline of automatic data generation.

Designer, responsible for formulating problems and assigning information to visual and textual modalities; (2) **Plotter**, which generates diagrams; (3) **Solver**, which provides answers and explanations; and (4) **Pair Constructor**, which produces four types of data and randomly selects two to form a data pair. Figure 2 illustrates this automatic data generation process.

- **Question Design:** The Question Designer employs a random selection process to determine the specific type of mathematical problem to be generated. It also randomly selects the information carrier, deciding whether to present the information as text or an image. This choice dictates the visual information sent to the Plotter and the textual information sent to the Solver.
- **Plotting:** In accordance with the visual information received, the Plotter uses the predefined fundamental tools to plot diagrams.
- **Problem Solving:** The Solver calculates the answer using the text-only version of the problem, which contains complete information. As the calculation is performed programmatically, the answer is reliable. Considering that MLLMs can obtain stronger reasoning abilities from step-by-step solutions, the Solver generates a detailed explanation for each problem by calling GPT-4o-mini (OpenAI 2024a) and verifying the explanations

against the standard answer to ensure accuracy.

- **Pair Construction:** The Pair Constructor combines the diagram from the Plotter and the text from the Solver to obtain up to four types of data, each comprising the same information but presented in a different modality: vision-only, vision-dominant, text-dominant, and text-only. Two of these are randomly selected to form a data pair, with the component containing more visual information classified as vision-rich and the other as text-rich.

We generated 40K data each for plane geometry, solid geometry, and functions, summing up to 120K.

Data Augmentation We initially collect 80K mathematical problem-solving data from online sources. By rephrasing the problems from multiple perspectives (Yu et al. 2023) and applying a series of traditional image processing techniques such as scaling, stretching, and gamma transformation, we expand the dataset to 310K. Additionally, we utilize the VisualWebInstruct dataset (TIGER-Lab 2024) containing 262K data. To automate the construction of data pairs, we employ a straightforward text-to-image rendering process to convert the content from textual to visual form. The original data serve as the text-rich component, while the generated data form the vision-rich component. In total, we obtain 572K data pairs.

Training Stages

We employ a three-stage pipeline to train our models, with specific details shown in Figure 3.

Stage 1: Enhancing the Language Model’s Mathematical Reasoning Abilities Given the abundance of unsupervised text-based mathematical training corpora and problem-solving data (Shao et al. 2024), in comparison to the scarcity of high-quality multimodal mathematical problem-solving data, we initially train the LLM on a large corpus of text-based math problems to bolster its mathematical reasoning capabilities. To leverage the strengths of existing LLMs that have demonstrated superior performance in mathematical problem-solving (Shao et al. 2024; Yang et al. 2024), we use them to initialize our MLLMs. Subsequently, we fine-tune the model using 200,000 data points extracted from various datasets (Yue et al. 2023; Tong et al. 2024; Mitra et al. 2024; LI et al. 2024). This phase significantly enhances the LLM’s mathematical reasoning abilities.

Stage 2: Progressive Upward Multimodal Alignment We observe that the multimodal mathematical reasoning ability of MLLMs resembles a pyramid, with performance declining from bottom to top as the information shifts from text to visual modalities. In order to address the discrepancy in performance between text-rich and vision-rich mathematical reasoning, we propose PUMA (Progressive Upward Multimodal Alignment). The objective of PUMA is to facilitate the effective resolution of vision-rich mathematical problems by aligning the outputs of MLLMs with text-rich data, thereby enhancing their reasoning capabilities across different modalities.

Let $i = 0, 1, 2, 3$ represents the levels of capability for MLLMs, ranging from weak to strong (top-down). For a vi-

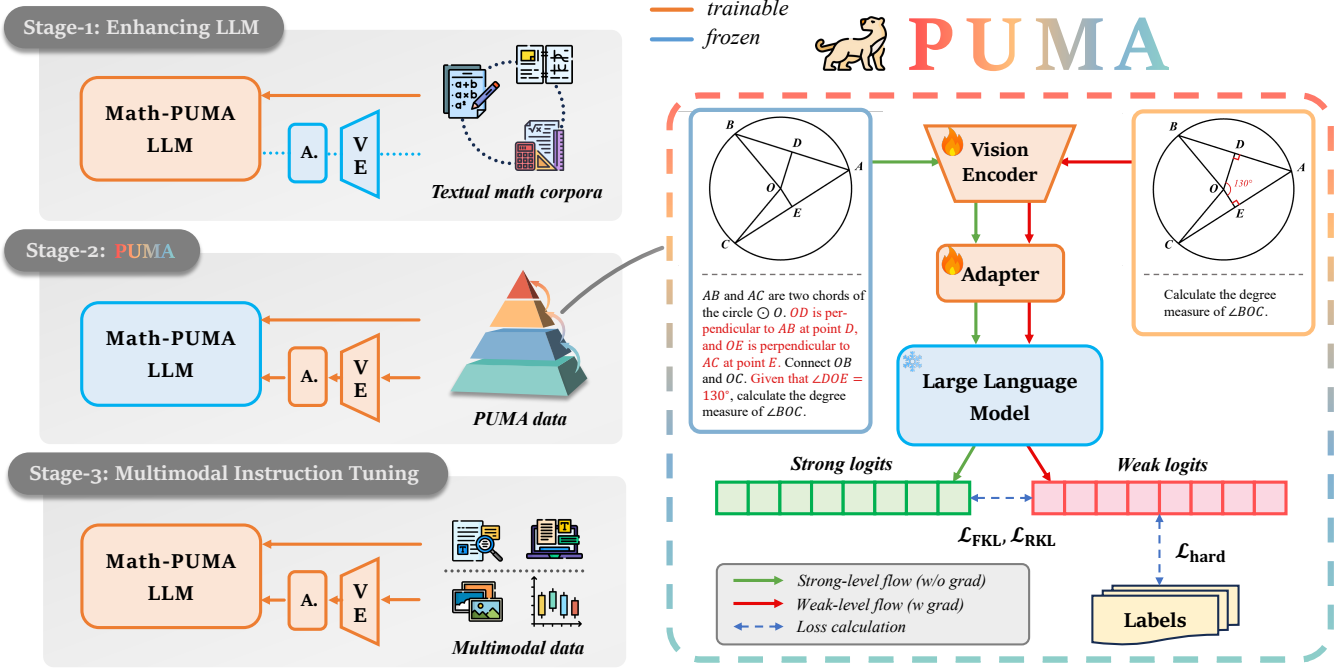


Figure 3: Overview of the Math-PUMA approach. (left) The three stage training process of Math-PUMA. (right) The details for aligning data pair. The input data pair includes text-rich data at the strong level and vision-rich data at the weak level, simultaneously processed by the MLLM. The strong logits and labels are used to supervise the weak logits.

sual mathematical problem, the inference results of MLLMs are progressively inferior on the i -th level compared to the $(i+1)$ -th level. We denote the response distribution (logits) obtained by MLLMs when processing the input of i -th level as p_i , while the response distribution (logits) obtained on the input of $(i+1)$ -th level is denoted as p_{i+1} . The forward KL (FKL) divergence and reverse KL (RKL) divergence between these distributions are calculated, since they converge to the same objective after a sufficient number of epochs for MLLMs (Wu et al. 2024).

Let $\mathbf{y}^{(i)} = \{y_t^{(i)}\}_{t=1}^T$ represent the response generated by MLLMs based on input $\mathbf{x}^{(i)}$. Here, $y_t^{(i)} \in \{Y_1^{(i)}, Y_2^{(i)}, \dots, Y_V^{(i)}\}$, with V representing the vocabulary size. p_i and p_{i+1} represent the distributions of weak and strong levels, $\mathbf{z}^{(i)} = (z_1^{(i)}, z_2^{(i)}, \dots, z_V^{(i)})$ and $\mathbf{z}^{(i+1)} = (z_1^{(i+1)}, z_2^{(i+1)}, \dots, z_V^{(i+1)})$ represent the logits of weak and strong levels, respectively. The FKL divergence and RKL divergence are computed as follows:

$$\begin{aligned} \mathcal{L}_{\text{FKL}} &= \frac{1}{TV} \sum_{t=1}^T \text{KL}(p_i(y_t^{(i)} | \mathbf{y}_{<t}^{(i)}) || p_{i+1}(y_t^{(i+1)} | \mathbf{y}_{<t}^{(i+1)})) \\ &= \frac{1}{TV} \sum_{t=1}^T \sum_{j=1}^V p_i(Y_j^{(i)} | \mathbf{y}_{<t}^{(i)}) \log \frac{p_i(Y_j^{(i)} | \mathbf{y}_{<t}^{(i)})}{p_{i+1}(Y_j^{(i+1)} | \mathbf{y}_{<t}^{(i+1)})}, \end{aligned} \quad (1)$$

$$\begin{aligned} \mathcal{L}_{\text{RKL}} &= \frac{1}{TV} \sum_{t=1}^T \text{KL}(p_{i+1}(y_t^{(i+1)} | \mathbf{y}_{<t}^{(i+1)}) || p_i(y_t^{(i)} | \mathbf{y}_{<t}^{(i)})) \\ &= \frac{1}{TV} \sum_{t=1}^T \sum_{j=1}^V p_{i+1}(Y_j^{(i+1)} | \mathbf{y}_{<t}^{(i+1)}) \log \frac{p_{i+1}(Y_j^{(i+1)} | \mathbf{y}_{<t}^{(i+1)})}{p_i(Y_j^{(i)} | \mathbf{y}_{<t}^{(i)})}, \end{aligned} \quad (2)$$

with

$$p_i(Y_j^{(i)} | \mathbf{y}_{<t}^{(i)}) = \frac{\exp(z_j^{(i)}/\tau)}{\sum_{k=1}^V \exp(z_k^{(i)}/\tau)}, \quad (3)$$

where τ represents the temperature hyperparameter.

Furthermore, to maintain training stability, we calculate a hard loss by utilizing the solutions of mathematical problems as the ground truth labels, i.e.,

$$\begin{aligned} \mathcal{L}_{\text{hard}} &= -\frac{1}{TV} \sum_{t=1}^T \log p_i(y_t^{(i)} | \mathbf{x}^{(i)}, \mathbf{y}_{<t}^{(i)}) \\ &= -\frac{1}{TV} \sum_{t=1}^T \sum_{j=1}^V \log p_i(Y_j^{(i)} | \mathbf{x}^{(i)}, \mathbf{y}_{<t}^{(i)}). \end{aligned} \quad (4)$$

Finally, the total loss is computed as

$$\mathcal{L} = \lambda_{\text{KL}}(\alpha_{\text{KL}}\mathcal{L}_{\text{FKL}} + (1 - \alpha_{\text{KL}})\mathcal{L}_{\text{RKL}})\tau^2 + (1 - \lambda_{\text{KL}})\mathcal{L}_{\text{hard}}, \quad (5)$$

where λ_{KL} is a hyperparameter that balances the weight between the combined FKL and RKL divergences and the hard loss term, α_{KL} is a weight hyperparameter that balances the contribution between \mathcal{L}_{FKL} and \mathcal{L}_{RKL} . The purpose of multiplying KL by τ^2 is to equalize the gradients of the two losses.

At this stage, we use a total of 692K data pairs for training, which includes 120K data pairs automatically generated and 572K data pairs obtained through data augmentation based on publicly available data as described in Data Construction.

Stage 3: Multimodal Instruction Tuning In the final phase, we enhance the model’s reasoning capabilities by incorporating multimodal problem-solving data. Initially, we retain the majority of the high-quality data used in Stage 2 and augment our dataset with the MathV360K dataset (Shi et al. 2024). Specifically, we focus on enriching the geometric problem subset within MathV360K, expanding it from 40K to 120K in order to address the scarcity of geometric data. Furthermore, we integrated a balanced amount of textual data to prevent any modal imbalance between text and visual modalities. All data included detailed reasoning processes to guide the model’s understanding and learning.

Ultimately, we compiled a large-scale instruction tuning dataset, comprising a total of 996K data points. This multimodal instruction tuning not only bolsters the model’s reasoning and problem-solving abilities but also ensures that it can effectively leverage both textual and visual information for improved performance in mathematical problem-solving.

Experiments

Experimental Setup

Models We validate the effectiveness of our method across various base models and scales, including DeepSeek-Math-7B (Shao et al. 2024), Qwen2-1.5B and Qwen2-7B (Yang et al. 2024), chosen as the LLM for Math-PUMA. To ensure the compatibility with DeepSeek-Math and DeepSeek-VL (Lu et al. 2024a), we adhere to the architecture of DeepSeek-VL. For Qwen2, we adopt a similar architecture to LLaVA, with the visual encoder designated as SigLIP-so400m-patch14-384 (Zhai et al. 2023).

Benchmarks We conduct extensive experiments on three popular multimodal mathematical problem-solving benchmarks: MATHVERSE (Zhang et al. 2024), MATHVISTA (Lu et al. 2024b), and WE-MATH (Qiao et al. 2024). MATHVERSE evaluates the multimodal mathematical reasoning abilities of MLLMs under five different conditions. MATHVISTA comprises samples that require fine-grained, in-depth visual understanding and compositional reasoning, posing a challenge for all baseline models on this benchmark. WE-MATH is the first benchmark specifically designed to explore the problem-solving principles beyond the end-to-end performance.

Evaluation and Metrics We refer to the leaderboards and adopt the official implementations of MATHVERSE, MATHVISTA, and WE-MATH. For MATHVERSE and MATHVISTA, initially, we use GPT-4o-mini (OpenAI 2024a) to extract answers from the responses generated by MLLMs. Subsequently, we employ GPT-4o-mini once more to verify the correctness of the extracted answers. The prompts used for answer extraction and correctness assessment are kept consistent with the official implementation. Ultimately, we calculate the accuracy scores as the evaluation metric. For WE-MATH, we select the average and Rote Memorization (RM) scores as evaluation metrics.

Implementation Details Our experiments are conducted using PyTorch version 2.1.0 and CUDA 12.1, utilizing 32

NVIDIA A100 GPUs with 80GB memory each. The training process is divided into three stages, each with specific hyperparameters and configurations. We employ the AdamW optimizer (Kingma and Ba 2014), configured with $\beta_1 = 0.9$ and $\beta_2 = 0.999$. The learning rate is adjusted across three stages: 3×10^{-5} for stage 1, 5×10^{-5} for stage 2, and 3×10^{-5} for stage 3. A cosine learning rate schedule is implemented with a warm-up phase covering 2% of the total training steps. Additionally, a decay rate of 0.1 is applied. The KL divergence is controlled using specific hyperparameters: α_{KL} is set to 0.2, τ to 1.0, and λ_{KL} to 0.1. The training is conducted over 1 epoch. The batch sizes for three stages are 256, 512, and 256, respectively.

Performance Comparison

Comparison on MATHVERSE MATHVERSE is capable of clearly demonstrating the gap between visual and textual modalities. From Table 1, it can be observed that the MLLMs trained by Math-PUMA achieve the state-of-the-art (SOTA) among open-source MLLMs. Compared to the previous SOTA method, Math-LLaVA, the MLLMs trained by Math-PUMA exhibit accuracy scores improvement about 10%. When compared to the closed-source GPT-4V (OpenAI 2023b), Math-PUMA-Qwen2-7B performs competitively with only a gap of 4.7%, demonstrating the effectiveness of Math-PUMA.

Comparison on MATHVISTA MATHVISTA is a comprehensive benchmark designed to evaluate mathematical reasoning. According to the results presented in Table 1, Math-PUMA-Qwen2-7B demonstrates SOTA performance in GPS, ALG, GEO and SCI domains among open-source MLLMs of the same scale. It outperforms InternLM-XComposer2-VL (Dong et al. 2024) by significant margins, with accuracy improvements of 16.4%, 15.7%, 16.8%, and 4.9% in these respective domains.

Comparison on WE-MATH WE-MATH places strong emphasis on the importance of the mathematical reasoning process. Table 2 demonstrates that Math-PUMA-Qwen2-7B achieves SOTA performance in average scores among open-source MLLMs with approximate 10B parameters, surpassing InternLM-XComposer2-VL. Notably, even among open-source MLLMs with parameters exceeding 20B, Math-PUMA-Qwen2-7B outperforms LLaVA-NeXT (Liu et al. 2024b) 72B model, reaching the performance of LLaVA-NeXT 110B model. While Math-PUMA-Qwen2-7B surpasses Qwen-VL-Max (Bai et al. 2023) among closed-source models, there remains a significant gap compared to GPT-4V and GPT-4o.

Ablation Study

Ablation studies are performed on MATHVERSE to highlight the contribution of each training stage and to assess the impact of their sequential order on Math-PUMA.

The Role of Each Stage To evaluate the significance of each stage, we conduct three ablation experiments by individually removing stages 1, 2, and 3. We then assess the

Table 1: **Mathematical evaluation on MATHVERSE and MATHVISTA *testmini* sets.** For MATHVERSE, we calculate the “ALL” score without averaging the “Text-only” version. For MATHVISTA, we select 4 mathematical categories from the original 12 categories. ALL: overall accuracy across original categories; GPS: geometry problem solving; ALG: algebraic reasoning; GEO: geometry reasoning; SCI: scientific reasoning. For closed-source and open-source MLLMs, the best accuracy scores are marked in **bold** fonts, while the second best accuracy scores are marked in underline fonts, respectively.

Model	# Params.	MATHVERSE						MATHVISTA				
		ALL \uparrow	Text-dom. \uparrow	Text-lite \uparrow	Vision-int. \uparrow	Vision-dom. \uparrow	Vision-only \uparrow	ALL \uparrow	GPS \uparrow	ALG \uparrow	GEO \uparrow	SCI \uparrow
<i>Baselines</i>												
Random chance	-	12.4	12.4	12.4	12.4	12.4	12.4	17.9	21.6	21.7	20.1	17.2
Human performance	-	64.9	71.2	70.9	61.4	68.3	66.7	60.3	48.4	50.9	51.4	64.9
<i>Closed-source LLMs</i>												
ChatGPT (Ouyang et al. 2022)	-	-	33.3	18.9	-	-	-	33.2	29.3	31.0	31.0	50.8
GPT-4 (OpenAI 2023a)	-	-	46.5	20.7	-	-	-	33.2	31.7	33.5	32.2	58.2
<i>Closed-source MLLMs</i>												
Qwen-VL-Plus (Bai et al. 2023)	-	11.8	15.7	11.1	9.0	13.0	10.0	43.3	38.5	39.1	39.3	59.0
Gemini-1.0-Pro (Gemini Team 2023)	-	22.3	27.6	23.7	19.4	20.3	20.5	45.2	40.4	45.2	41.0	54.9
Qwen-VL-Max (Bai et al. 2023)	-	24.8	30.3	24.8	20.6	23.3	25.1	-	-	-	-	-
GPT-4V (OpenAI 2023b)	-	38.3	52.1	40.9	34.9	33.6	29.8	49.9	50.5	53.0	51.0	63.1
<i>Open-source MLLMs</i>												
mPLUG-Owl2 (Ye et al. 2024)	7B	4.6	6.6	6.3	6.3	5.6	4.9	22.2	23.6	23.6	23.9	26.3
LLaMA-Adapter-V2 (Gao et al. 2023b)	7B	5.7	6.2	5.9	6.1	4.2	6.1	23.9	25.5	26.3	24.3	29.5
LLaVA-1.5 (Liu et al. 2024a)	13B	7.6	8.8	7.6	7.4	7.4	6.9	25.7	18.3	19.6	17.6	42.6
LLaVA-NeXT (Liu et al. 2024b)	8B	10.3	12.8	12.0	10.7	9.7	6.3	34.6	-	-	-	-
MiniGPT-v2 (Chen et al. 2023a)	7B	11.0	12.1	12.0	13.1	10.3	7.4	23.1	26.0	28.1	24.7	25.4
SPHINX-Plus (Gao et al. 2024)	13B	12.2	13.9	11.6	11.6	13.5	10.4	36.8	-	-	-	-
ShareGPT4V (Chen et al. 2023b)	13B	13.1	16.2	16.2	15.5	13.8	3.7	27.5	27.4	-	27.6	-
InternLM-XC2. (Dong et al. 2024)	7B	16.3	20.2	14.3	14.2	17.5	15.2	<u>47.8</u>	31.7	32.0	30.5	37.7
G-LLaVA (Gao et al. 2023a)	7B	16.6	20.9	20.7	17.2	14.6	9.4	23.8	38.9	36.3	35.6	20.5
SPHINX-MoE (Gao et al. 2024)	8×7B	16.8	26.2	17.4	16.7	12.5	11.1	42.3	31.2	31.7	30.5	50.8
DeepSeek-VL (Lu et al. 2024a)	7B	19.3	23.0	23.2	20.2	18.4	11.8	34.9	28.4	29.2	27.2	35.3
Math-LLaVA (Shi et al. 2024)	13B	22.9	27.3	24.9	24.5	21.7	16.1	38.3	29.3	28.5	30.5	42.6
Math-PUMA-Qwen2-1.5B	1.5B	29.6	35.8	32.2	31.3	<u>30.4</u>	18.5	44.5	<u>47.6</u>	<u>43.4</u>	47.3	41.0
Math-PUMA-Qwen2-7B	7B	33.6	<u>42.1</u>	<u>35.0</u>	<u>33.4</u>	31.6	26.0	47.9	48.1	47.7	47.3	42.6
Math-PUMA-DeepSeek-Math-7B	7B	<u>31.8</u>	43.4	35.4	33.6	31.6	14.7	44.7	39.9	39.2	<u>41.4</u>	<u>48.4</u>

accuracy across overall, text-dominant, and vision-only scenarios, as well as the gaps between them. The results of these experiments are summarized in Table 3.

Removing Stage 1: Stage 1 aims to enhance the mathematical reasoning capabilities of the LLMs. As observed in Table 3, upon removing stage 1, there is a slight decrease in the accuracy compared to the corresponding model trained with all three stages. This reduction occurs because stage 1 serves as the foundation for stage 2. When the LLM lacks strong mathematical reasoning capabilities, strong logits are not reliable to supervise weak logits, resulting in lower performance. However, due to the presence of complete stage 2 and 3, the gap remains close to that of the complete three-stage training model and relatively low.

Removing Stage 2: Stage 2 embodies our devised PUMA, facilitating a close alignment between visual and textual modalities. As depicted in Table 3, the absence of stage 2 results in a wider gap in reasoning performance between textual and visual modalities when compared to the three-stage approach. Nonetheless, with the enhancement of mathematical reasoning capabilities by stage 1 and multimodal instruction tuning with high-quality data through stage 3, the overall performance persists at a relatively high level.

Removing Stage 3: Stage 3 is multimodal instruction tuning. We observe that if only stage 1 and 2 are performed without subsequent multimodal instruction tuning, MLLMs tend to lose conversational capabilities to some extent. As seen in Table 3, the performance of MLLMs drastically declines when stage 3 is excluded, primarily due to the loss of conversational capabilities. Since we have conducted stage 2, the gap between textual and visual modalities remains relatively small.

Sequential Order of Stages We swap stage 2 and 3 to assess their impact on MLLMs. As shown in Table 3, exchanging stage 2 and 3 leads to a significant performance drop. Our analysis of each stage reveals the critical role of stage 3 in maintaining the conversational abilities of MLLMs. Consequently, rearranging the stage 2 and 3 results in the loss of conversational skills of MLLMs, thereby influencing their overall performance. Nonetheless, the eventual implementation of stage 2 ensures that the gap between textual and visual modalities remains relatively small.

Have the modality gaps truly narrowed? Through the aforementioned analysis, we have demonstrated the efficacy of our method. However, we still seek to provide a definitive conclusion to address the initial query: Has the perfor-

Table 2: **Evaluation results on WE-MATH *testmini* set.** AVG: average score (strict); RM: rote memorization (strict). The best scores of each category are marked in **bold** fonts.

Model	# Params.	AVG \uparrow	RM \downarrow
<i>Closed-source MLLMs</i>			
Qwen-VL-Max (Bai et al. 2023)	-	10.5	75.5
Gemini-1.5-Pro (Reid et al. 2024)	-	26.4	54.8
GPT-4V (OpenAI 2023b)	-	31.1	47.9
GPT-4o (OpenAI 2024b)	-	42.9	34.2
<i>Open-source MLLMs ($\geq 20B$)</i>			
InternVL-Chat-V1.5 (Chen et al. 2024)	26B	15.0	73.3
LLaVA-NeXT (Liu et al. 2024b)	72B	13.4	71.0
LLaVA-NeXT (Liu et al. 2024b)	110B	19.2	66.0
<i>Open-source MLLMs ($\approx 10B$)</i>			
LLaVA-1.5 (Liu et al. 2024a)	7B	6.5	85.6
LLaVA-1.5 (Liu et al. 2024a)	13B	8.4	78.1
LLaVA-1.6 (Liu et al. 2024b)	7B	3.3	89.1
LLaVA-1.6 (Liu et al. 2024b)	13B	5.2	86.9
DeepSeek-VL (Lu et al. 2024a)	7B	6.3	84.8
G-LLaVA (Gao et al. 2023a)	13B	6.5	86.6
Math-LLaVA (Shi et al. 2024)	13B	11.1	72.8
InternLM-XC2. (Dong et al. 2024)	7B	12.7	77.6
Math-PUMA-Qwen2-1.5B	1.5B	10.4	75.5
Math-PUMA-Qwen2-7B	7B	19.2	67.8
Math-PUMA-DeepSeek-Math	7B	15.6	67.4

Table 3: **Results of ablation study.** Order: the sequential order of Stage 1, 2, and 3; ALL: overall accuracy; Text-dom.: accuracy of text-dominant data; Vision-only: accuracy of vision-only data; Gap: (Text-dom. – Vision-only) / Vision-only. The best scores of each LLM are marked in **bold** fonts.

Order	LLM	ALL \uparrow	Text-dom. \uparrow	Vision-only \uparrow	Gap \downarrow
<i>Standard pipeline</i>					
1 \rightarrow 2 \rightarrow 3	Qwen2-1.5B	29.6	35.8	18.5	93.5
	Qwen2-7B	33.6	42.1	26.0	61.9
	DeepSeek-Math	31.8	43.4	14.7	195.2
<i>Effectiveness of Stage 1 (Enhancing LLM)</i>					
2 \rightarrow 3	Qwen2-1.5B	17.0	19.9	12.1	64.5
	Qwen2-7B	19.6	27.3	11.9	129.4
	DeepSeek-Math	23.9	30.7	11.2	174.1
<i>Effectiveness of Stage 2 (Math-PUMA)</i>					
1 \rightarrow 3	Qwen2-1.5B	24.6	40.3	9.8	311.2
	Qwen2-7B	27.2	44.1	11.0	300.9
	DeepSeek-Math	29.3	43.4	9.1	376.9
<i>Effectiveness of Stage 3 (Multimodal instruction tuning)</i>					
1 \rightarrow 2	Qwen2-1.5B	11.7	15.5	8.1	91.4
	Qwen2-7B	21.2	28.9	12.2	136.9
	DeepSeek-Math	22.2	36.2	14.8	144.6
<i>Sequential Order of Stages</i>					
1 \rightarrow 3 \rightarrow 2	Qwen2-1.5B	24.5	38.2	12.1	215.7
	Qwen2-7B	26.7	34.4	18.7	84.0
	DeepSeek-Math	23.4	34.3	4.3	697.7

mance gap between different modalities truly narrowed? To this end, we base our exploration on the evaluation metrics provided by MATHVERSE, calculating the average scores of the model on text-based questions and visual questions to

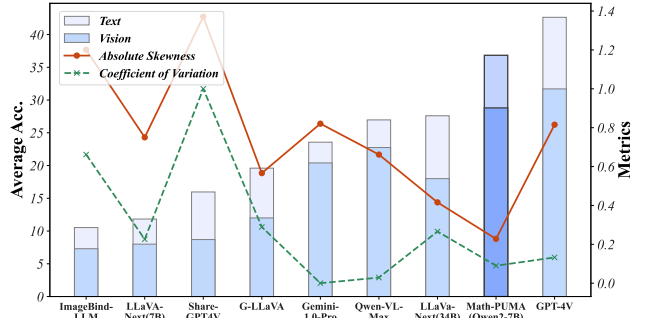


Figure 4: Visualizing MLLMs’ Performance on MATHVERSE. “Text” represents the average scores for text-dominant and text-lite categories, while “Vision” represents the average scores for vision-intensive, vision-dominant, and vision-only categories. “Absolute Skewness” and “Coefficient of Variance” denote the statistical measures of score distribution across the five categories, with skewness taken as an absolute value.

intuitively assess the model’s performance across these two distinct modalities. Additionally, we compute the skewness and coefficient of variation of the model’s scores on different types of questions in MATHVERSE to corroborate our observations regarding the model’s modal balance.

As illustrated in Figure 4, we compare our model, trained using our proposed method, with several popular MLLMs. In terms of overall performance, our model attains high average scores on both text and image-based questions, outperforming closed-source MLLMs such as Gemini-1.0-Pro and Qwen-VL-Max. We analyze the performance gap between text and visual modalities. Our model maintains a high level of performance while exhibiting a relatively smaller gap, which is even less than that of GPT-4V. Additionally, regarding score distribution, a model that performs consistently across modalities should demonstrate similar scores across various types of questions in MATHVERSE. Such consistency is indicated by lower absolute skewness and coefficient of variation. By visualizing the score distributions of multiple models, it is evident that our model exhibits low levels of both skewness and coefficient of variation, indicating a well-balanced performance across different types. In summary, our alignment method effectively mitigates the performance disparity between different modalities.

Conclusion

In this paper, we present Math-PUMA, a progressive upward multimodal alignment approach aimed at enhancing the mathematical reasoning capabilities of MLLMs. Experimental results indicate that Math-PUMA MLLMs not only achieve state-of-the-art performance among open-source models on multiple mathematical benchmarks but also significantly reduce the performance gap between textual and visual modalities. Despite the impressive results of Math-PUMA, a undeniable disparity remains when compared to human-level proficiency. Continued exploration in high-

quality data augmentation, automated data generation methods, and effective training strategies is necessary to further advance the mathematical reasoning abilities of MLLMs. We hope our work provides valuable insights and inspiration for future research in this domain.

References

- Bai, J.; Bai, S.; Yang, S.; Wang, S.; Tan, S.; Wang, P.; Lin, J.; Zhou, C.; and Zhou, J. 2023. Qwen-VL: A Frontier Large Vision-Language Model with Versatile Abilities. *arXiv preprint arXiv:2308.12966*.
- Cai, S.; Bao, K.; Guo, H.; Zhang, J.; Song, J.; and Zheng, B. 2024. GeoGPT4V: Towards Geometric Multi-modal Large Language Models with Geometric Image Generation. *arXiv preprint arXiv:2406.11503*.
- Chen, J.; Li, D. Z. X. S. X.; Zhang, Z. L. P.; Xiong, R. K. V. C. Y.; and Elhoseiny, M. 2023a. MiniGPT-V2: Large Language Model as a Unified Interface for Vision-Language Multi-task Learning. *arXiv preprint arXiv:2310.09478*.
- Chen, L.; Li, J.; wen Dong, X.; Zhang, P.; He, C.; Wang, J.; Zhao, F.; and Lin, D. 2023b. ShareGPT4V: Improving Large Multi-Modal Models with Better Captions. *ArXiv, abs/2311.12793*.
- Chen, W.; Ma, X.; Wang, X.; and Cohen, W. W. 2022. Program of thoughts prompting: Disentangling computation from reasoning for numerical reasoning tasks. *arXiv preprint arXiv:2211.12588*.
- Chen, Z.; Wang, W.; Tian, H.; Ye, S.; Gao, Z.; Cui, E.; Tong, W.; Hu, K.; Luo, J.; Ma, Z.; et al. 2024. How Far Are We to GPT-4V? Closing the Gap to Commercial Multimodal Models with Open-Source Suites. *arXiv preprint arXiv:2404.16821*.
- Dong, X.; Zhang, P.; Zang, Y.; Cao, Y.; Wang, B.; Ouyang, L.; Wei, X.; Zhang, S.; Duan, H.; Cao, M.; et al. 2024. InternLM-XComposer2: Mastering free-form text-image composition and comprehension in vision-language large model. *arXiv preprint arXiv:2401.16420*.
- Gao, J.; Pi, R.; Zhang, J.; Ye, J.; Zhong, W.; Wang, Y.; Hong, L.; Han, J.; Xu, H.; Li, Z.; et al. 2023a. G-LLaVA: Solving Geometric Problem with Multi-Modal Large Language Model. *arXiv preprint arXiv:2312.11370*.
- Gao, P.; Han, J.; Zhang, R.; Lin, Z.; Geng, S.; Zhou, A.; Zhang, W.; Lu, P.; He, C.; Yue, X.; Li, H.; and Qiao, Y. 2023b. LLaMA-Adapter V2: Parameter-Efficient Visual Instruction Model. *arXiv preprint arXiv:2304.15010*.
- Gao, P.; Zhang, R.; Liu, C.; Qiu, L.; Huang, S.; Lin, W.; Zhao, S.; Geng, S.; Lin, Z.; Jin, P.; et al. 2024. SPHINX-X: Scaling Data and Parameters for a Family of Multi-modal Large Language Models. *arXiv preprint arXiv:2402.05935*.
- Gemini Team, G. 2023. Gemini: a family of highly capable multimodal models. *arXiv preprint arXiv:2312.11805*.
- Gou, Z.; Shao, Z.; Gong, Y.; Yang, Y.; Huang, M.; Duan, N.; Chen, W.; et al. 2023. Tora: A tool-integrated reasoning agent for mathematical problem solving. *arXiv preprint arXiv:2309.17452*.
- Kingma, D. P.; and Ba, J. 2014. Adam: A method for stochastic optimization. *arXiv preprint arXiv:1412.6980*.
- LI, J.; Beeching, E.; Tunstall, L.; Lipkin, B.; Soletskyi, R.; Huang, S. C.; Rasul, K.; Yu, L.; Jiang, A.; Shen, Z.; Qin, Z.; Dong, B.; Zhou, L.; Fleureau, Y.; Lample, G.; and Polu, S. 2024. NuminaMath. <https://huggingface.co/AI-MO/NuminaMath-CoT>.
- Li, J.; Li, D.; Xiong, C.; and Hoi, S. 2022. Blip: Bootstrapping language-image pre-training for unified vision-language understanding and generation. In *International conference on machine learning*, 12888–12900. PMLR.
- Liu, H.; Li, C.; Li, Y.; and Lee, Y. J. 2024a. Improved baselines with visual instruction tuning. In *Proceedings of the IEEE/CVF Conference on Computer Vision and Pattern Recognition*, 26296–26306.
- Liu, H.; Li, C.; Li, Y.; Li, B.; Zhang, Y.; Shen, S.; and Lee, Y. J. 2024b. LLaVA-NeXT: Improved Reasoning, OCR, and World Knowledge.
- Liu, H.; Li, C.; Wu, Q.; and Lee, Y. J. 2023. Visual Instruction Tuning. In *NeurIPS*.
- Liu, H.; and Yao, A. C.-C. 2024. Augmenting math word problems via iterative question composing. *arXiv preprint arXiv:2401.09003*.
- Lu, H.; Liu, W.; Zhang, B.; Wang, B.; Dong, K.; Liu, B.; Sun, J.; Ren, T.; Li, Z.; Sun, Y.; et al. 2024a. Deepseek-VL: Towards Real-world Vision-Language Understanding. *arXiv preprint arXiv:2403.05525*.
- Lu, P.; Bansal, H.; Xia, T.; Liu, J.; Li, C.; Hajishirzi, H.; Cheng, H.; Chang, K.-W.; Galley, M.; and Gao, J. 2024b. MathVista: Evaluating Mathematical Reasoning of Foundation Models in Visual Contexts. In *The Twelfth International Conference on Learning Representations*.
- Mitra, A.; Khanpour, H.; Rosset, C.; and Awadallah, A. 2024. Orca-math: Unlocking the potential of slms in grade school math. *arXiv preprint arXiv:2402.14830*.
- OpenAI. 2023a. GPT-4 Technical Report. *ArXiv, abs/2303.08774*.
- OpenAI. 2023b. GPT-4V(ision) System Card.
- OpenAI. 2024a. GPT-4o mini: advancing cost-efficient intelligence.
- OpenAI. 2024b. GPT-4o System Card.
- Ouyang, L.; Wu, J.; Jiang, X.; Almeida, D.; Wainwright, C.; Mishkin, P.; Zhang, C.; Agarwal, S.; Slama, K.; Gray, A.; Schulman, J.; Hilton, J.; Kelton, F.; Miller, L.; Simens, M.; Askell, A.; Welinder, P.; Christiano, P.; Leike, J.; and Lowe, R. 2022. Training language models to follow instructions with human feedback. In *Advances in Neural Information Processing Systems*.
- Qiao, R.; Tan, Q.; Dong, G.; Wu, M.; Sun, C.; Song, X.; GongQue, Z.; Lei, S.; Wei, Z.; Zhang, M.; et al. 2024. We-Math: Does Your Large Multimodal Model Achieve Human-like Mathematical Reasoning? *arXiv preprint arXiv:2407.01284*.
- Radford, A.; Kim, J. W.; Hallacy, C.; Ramesh, A.; Goh, G.; Agarwal, S.; Sastry, G.; Askell, A.; Mishkin, P.; Clark, J.;

et al. 2021. Learning Transferable Visual Models from Natural Language Supervision. In *International conference on machine learning*, 8748–8763. PMLR.

Reid, M.; Savinov, N.; Teplyashin, D.; Lepikhin, D.; Lillcrap, T.; Alayrac, J.-b.; Soricut, R.; Lazaridou, A.; Firat, O.; Schrittwieser, J.; et al. 2024. Gemini 1.5: Unlocking multimodal understanding across millions of tokens of context. *arXiv preprint arXiv:2403.05530*.

Saxton, D.; Grefenstette, E.; Hill, F.; and Kohli, P. 2019. Analysing mathematical reasoning abilities of neural models. *arXiv preprint arXiv:1904.01557*.

Shao, Z.; Wang, P.; Zhu, Q.; Xu, R.; Song, J.; Zhang, M.; Li, Y.; Wu, Y.; and Guo, D. 2024. DeepSeekMath: Pushing the Limits of Mathematical Reasoning in Open Language Models. *arXiv preprint arXiv:2402.03300*.

Shi, W.; Hu, Z.; Bin, Y.; Liu, J.; Yang, Y.; Ng, S.-K.; Bing, L.; and Lee, R. K.-W. 2024. Math-LLaVA: Bootstrapping Mathematical Reasoning for Multimodal Large Language Models. *arXiv preprint arXiv:2406.17294*.

TIGER-Lab. 2024. VisualWebInstruct.

Tong, Y.; Zhang, X.; Wang, R.; Wu, R.; and He, J. 2024. DART-Math: Difficulty-Aware Rejection Tuning for Mathematical Problem-Solving. *arXiv preprint arXiv:2407.13690*.

Wei, J.; Wang, X.; Schuurmans, D.; Bosma, M.; Xia, F.; Chi, E.; Le, Q. V.; Zhou, D.; et al. 2022. Chain-of-thought prompting elicits reasoning in large language models. *Advances in neural information processing systems*, 35: 24824–24837.

Wu, T.; Tao, C.; Wang, J.; Zhao, Z.; and Wong, N. 2024. Rethinking Kullback-Leibler Divergence in Knowledge Distillation for Large Language Models. *arXiv preprint arXiv:2404.02657*.

Yang, A.; Yang, B.; Hui, B.; Zheng, B.; Yu, B.; Zhou, C.; Li, C.; Li, C.; Liu, D.; Huang, F.; et al. 2024. Qwen2 technical report. *arXiv preprint arXiv:2407.10671*.

Ye, Q.; Xu, H.; Ye, J.; Yan, M.; Hu, A.; Liu, H.; Qian, Q.; Zhang, J.; and Huang, F. 2024. mPLUG-Owl2: Revolutionizing Multi-modal Large Language Model with Modality Collaboration. In *Proceedings of the IEEE/CVF Conference on Computer Vision and Pattern Recognition*, 13040–13051.

Yu, L.; Jiang, W.; Shi, H.; Yu, J.; Liu, Z.; Zhang, Y.; Kwok, J. T.; Li, Z.; Weller, A.; and Liu, W. 2023. Metamath: Bootstrap your own mathematical questions for large language models. *arXiv preprint arXiv:2309.12284*.

Yue, X.; Qu, X.; Zhang, G.; Fu, Y.; Huang, W.; Sun, H.; Su, Y.; and Chen, W. 2023. Mammoth: Building math generalist models through hybrid instruction tuning. *arXiv preprint arXiv:2309.05653*.

Zhai, X.; Mustafa, B.; Kolesnikov, A.; and Beyer, L. 2023. Sigmoid loss for language image pre-training. In *Proceedings of the IEEE/CVF International Conference on Computer Vision*, 11975–11986.

Zhang, R.; Jiang, D.; Zhang, Y.; Lin, H.; Guo, Z.; Qiu, P.; Zhou, A.; Lu, P.; Chang, K.-W.; Gao, P.; et al. 2024. MathVerse: Does Your Multi-modal LLM Truly See the Diagrams in Visual Math Problems? *arXiv preprint arXiv:2403.14624*.

Details of Automatic Data Generation

We provide implementation details of automatic data generation for three major types of mathematical problems as follows:

- **Plane Geometry:** Triangles, quadrilaterals, and circles are the primary elements for plane geometry. Taking triangles as an example. Initially, the Question Designer constructs problems using the three basic known conditions as premises. Subsequently, the Solver for triangles utilizes these known conditions to determine all the other properties of the triangle. The Solver leverages sine and cosine rules for calculating all the properties of a triangle, including sides, angles, perimeter, and area, by providing at least three basic known conditions: side-side-side (SSS), side-angle-side (SAS), angle-side-angle (ASA), or angle-angle-side (AAS). Moreover, the Solver enriches the problem-solving process through GPT-4o-mini. Finally, the Plotter plots the triangle and sends it to the Pair Constructor for assembly into a data pair.
- **Solid Geometry:** We focus on five distinctive solid geometric shapes, including cylinders, cones, prisms, pyramids, and spheres. Random values for the base radius and height are assigned for cylinders and cones, while for prisms and pyramids, random values for the length of base sides and height are given. As for spheres, only the radius is randomized.
- **Functions:** We focus on six primary function types, i.e., polynomial, absolute value, logarithmic, sine, cosine, and tangent functions. Initially, we develop a tool for the Plotter that enables the plotting of function graphs based on user input of the function type and parameters. Next, the Question Designer generate a variety of functions by randomly selecting the function type and parameters. Subsequently, the Question Designer utilize specific details to formulate problem statements while reserving other information for the problem-solving process. For example, given that a function passes through multiple points, we aim to determine the function’s expression and properties such as zeros, symmetry axis, and period.

Training Datasets Details

A diverse and extensive dataset is the most crucial element of MLLM training. Our dataset can be divided into three parts: 200K text-only supervised fine-tuning data for stage 1, 692K alignment data pairs for stage 2 and 996K multimodal instruction tuning data for stage 3.

Stage 1

We extract 200K data from the existing four datasets for supervised fine-tuning of the LLM. The detailed descriptions of the four sources are as follows:

- **DART-Math-Hard (Tong et al. 2024)** comprises approximately 585K mathematical question-answer pairs, generated by using DARS-Prop2Diff on the query sets from the MATH and GSK8K training datasets. This dataset attains state-of-the-art performance on several demanding mathematical reasoning benchmarks. Unlike stan-

standard rejection sampling, it intentionally emphasizes difficult queries.

- **Orca-Math-dataset** (Mitra et al. 2024) is a high-quality synthetic dataset comprising 200K math problems. This dataset was meticulously crafted using an innovative multi-agent setup, known as Agent-Instruct, where agents work collaboratively to generate and enhance the data. Each problem is paired with solutions generated by Azure GPT-4 Turbo, ensuring both accuracy and comprehensiveness.
- **NuminaMath-CoT** (LI et al. 2024) includes approximately 860K math problems, each accompanied by a Chain of Thought solution. This dataset spans a spectrum of difficulties, from Chinese high school exercises to international mathematics olympiad challenges. The NuminaMath-CoT dataset aims to enhance the mathematical reasoning prowess of LLMs through the CoT approach.
- **MathInstruct** (Yue et al. 2023) is a meticulously curated instruction tuning dataset designed to be both lightweight and highly generalizable. Compiled from 13 different math rationale datasets, including six newly curated specifically for this work, MathInstruct stands out for its unique focus on the hybrid use of chain-of-thought and program-of-thought rationales, with 262K math problems. This approach ensures extensive coverage across a wide range of mathematical fields, making it an invaluable resource for diverse mathematical problem-solving and instruction tuning.

Stage 2

We construct 692K data pairs, each pair conveying identical information but differing in multimodal representation to enhance multimodal alignment. The methods we employ to construct data pairs include automatic data generation and data augmentation based on publicly available sources. Figure 6 illustrates a few examples.

- **Automatically Generated Dataset** includes 120K data pairs using an automated data generation pipeline, with multiple agents working collaboratively. The dataset encompasses three major categories: planar geometry, solid geometry, and functions.
- **Manually collecting** 80K data from online sources and augmented it to 310K using question rephrasing and image transformation methods. To streamline the creation of data pairs, we utilize a simple text-to-image rendering technique to convert the content from textual to visual form. The initial data act as the text-rich component, while the produced data form the vision-rich component.
- **VisualWebInstruct** dataset (TIGER-Lab 2024) comprises 262K data with science images. Corresponding question-answer pairs are generated with large language models like GPT-4o, GPT-4v, Gemini for each image. We use the same method to construct the data pairs.

Stage 3

We select 996K high-quality multimodal problem-solving data to fine-tune the model, further enhancing its perfor-

mance in multimodal mathematical problem-solving tasks. The data sources are as follows. Figure 7 shows some examples.

- **MathV360K** (Shi et al. 2024) consists of 40K images from 24 different datasets and includes 360K question-answer pairs. It is specifically designed to enhance the multimodal mathematical reasoning capabilities of MLLMs. We enrich the geometric problem subset within MathV360K, expanding it from 40K to 120K to address the scarcity of geometric data.
- **VisualWebInstruct**. Using the same source as Stage 2, only the original data is used here, not the data pairs.
- **Manually collected dataset**. Using the same source as Stage 2, only the original data is used here, not the data pairs.

Implementation Details

Environment

The experiment utilizes the following libraries and their respective versions: torch=2.1.0, CUDA_version=12.1, transformers=4.42.0, datasets=2.18.0, tqdm=4.40.0, Pillow=9.3.0, loguru=0.7.0.

Hardware Configurations

The experiments are conducted using 32 NVIDIA A100 GPUs with 80GB memory each.

Hyperparameters Details

The training process is divided into 3 stages, each with specific settings tailored to optimize performance. The detailed hyperparameters of all stages are summarized in Table 4.

Table 4: Detailed hyperparameters of our models.

Hyperparameters	Stage 1	Stage 2	Stage 3
Learning rate	3×10^{-5}	5×10^{-5}	3×10^{-5}
LR scheduler	Cosine	Cosine	Cosine
Weight decay	0.1	0.05	0.1
Gradient clip	1.0	1.0	1.0
Optimizer	AdamW ($\beta_1 = 0.9, \beta_2 = 0.999$)		
Warm-up ratio	0.02	0.02	0.02
training data quantity	200K	692K	996K
Batch size	256	512	256
Sequence length	2048	2048	2048
Mixed precision training	BF16	BF16	BF16

Competitors Details

In this section, we provide a comprehensive overview of the various models that serve as competitors in our comparative analysis. These models are categorized into three main groups: closed-source LLMs, closed-source MLLMs, and open-source MLLMs.

Closed-source LLMs

- **ChatGPT** (Ouyang et al. 2022) is developed by OpenAI. ChatGPT is a highly versatile conversational agent based on the GPT-3 architecture.
- **GPT-4** (OpenAI 2023a) is also developed by OpenAI. GPT-4 is the successor to GPT-3, offering significant improvements in terms of language understanding and generation capabilities.

Closed-source MLLM

- **Qwen-VL-Plus** (Bai et al. 2023) and **Qwen-VL-Max** (Bai et al. 2023): The Qwen-VL series introduces a new visual receptor, which incorporates a language-aligned visual encoder and a position-aware adapter, significantly enhancing its ability to perceive and understand visual inputs. The Qwen-VL-Plus and Qwen-VL-Max, as part of this series, stand as the enhanced and the most capable large visual language model, respectively.
- **Gemini-1.0-Pro** (Gemini Team 2023) is developed by Google. It is designed to handle a wide range of tasks with impressive capabilities. Gemini-1.0-Pro is a member of the Gemini family. The Pro version is particularly balanced in terms of performance and efficiency, making it suitable for a broad spectrum of uses.
- **GPT-4V** (OpenAI 2023b) is the multimodal extension of GPT-4 by OpenAI, capable of processing both text and visual data.

Open-source MLLMs

- **mPLUG-Owl2** (Ye et al. 2024) features a modularized network design with a language decoder that acts as a universal interface for managing different modalities, incorporating shared functional modules and a modality-adaptive module to facilitate cross-modality interaction while preserving modality-specific features.
- **LLaMA-Adapter-V2** (Gao et al. 2023b) is an upgrade to LLMs, enabling them to process visual data alongside text efficiently. It introduces new learnable parameters, fuses visual information early in the model, and uses a specialized joint training technique. The model leverages expert systems for enhanced image comprehension, all with minimal additional training costs.
- **LLaVA-1.5** (Liu et al. 2024a) and **LLaVA-NeXT** (Liu et al. 2024b): LLaVA series utilize a simple mlp to connect the vision encoder and LLM. LLaVA-1.5 is the improved version of the LLaVA model, designed for better performance in multimodal tasks. LLaVA-NeXT is the latest iteration in the LLaVA series, offering enhanced multimodal capabilities and improved performance.
- **MiniGPT-v2** (Chen et al. 2023a) aims to serve as a unified interface for a variety of vision-language tasks. It utilizes unique identifiers for different tasks during training, enhancing the model’s ability to distinguish and efficiently learn each task.
- **SPHINX-Plus** (Gao et al. 2024) is a member of the SPHINX-X family, leverages the robust LLaMA2-13B

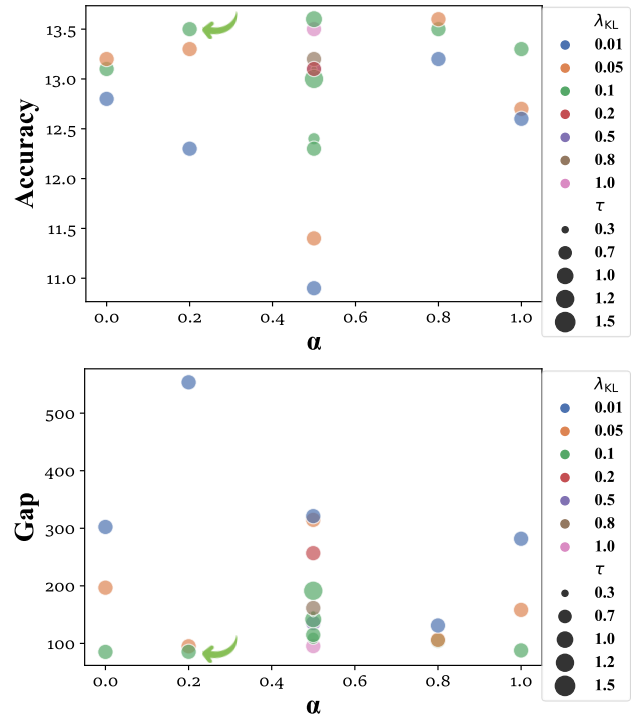


Figure 5: Visualizing hyperparameter choices, accuracy scores, and gaps on MATHVERSE. The X-axis represents α , while the Y-axes of the top and bottom sub-figures show accuracy scores and gaps, respectively. The bubble color indicates λ_{KL} , and the bubble size corresponds to τ . The green arrow represents our final hyperparameter choice.

base language model. It is meticulously engineered to amplify visual and linguistic comprehension.

- **ShareGPT4V** (Chen et al. 2023b) is a novel large-scale multi-modal model that significantly enhances the alignment of vision and language modalities by leveraging a dataset of 1.2M highly descriptive image captions. These captions are generated using advanced GPT4-Vision technology, resulting in detailed and accurate descriptions that cover a wide range of information
- **InternLM-XComposer2** (Dong et al. 2024) effortlessly integrates sophisticated comprehension and creation of text-image content, transforming the way we interact with vision-language and providing fresh perspectives and possibilities.
- **G-LLaVA** (Gao et al. 2023a) leverages a dataset called Geo170K, which contains over 170K meticulously crafted geometric image-caption and question-answer pairs, to significantly enhance LLaVA’s ability to interpret geometric figures and solve related problems.
- **SPHINX-MoE** (Gao et al. 2024) is a prominent member of the SPHINX-X family. It integrates a sparse Mixture-of-Experts (MoE) architecture with 8 experts per layer, allowing it to efficiently scale up to a large parameter size without a proportional increase in computational costs.

- **DeepSeek-VL** (Lu et al. 2024a) utilizes a hybrid vision encoder, specifically engineered to manage high-resolution images within a predetermined token limit, ensuring the model’s proficiency in discerning vital semantic and complex details across a range of visual tasks.
- **Math-LLaVA** (Shi et al. 2024) is an enhanced version of the LLaVA-1.5 model, fine-tuned with a novel dataset called MathV360K. This dataset consists of 40K high-quality images with question-answer pairs and an additional 320K synthesized pairs to improve multimodal mathematical reasoning capabilities.

Sensitivity Analysis of Hyperparameters

We use different combinations of hyperparameters to train MLLMs, then evaluate them on MATHVERSE. The loss is computed as

$$\mathcal{L} = \lambda_{\text{KL}}(\alpha_{\text{KL}}\mathcal{L}_{\text{FKL}} + (1 - \alpha_{\text{KL}})\mathcal{L}_{\text{RKL}})\tau^2 + (1 - \lambda_{\text{KL}})\mathcal{L}_{\text{hard}}, \quad (6)$$

where λ_{KL} is a hyperparameter that balances the weight between the combined FKL and RKL and the hard loss term, α_{KL} is a weight hyperparameter that balances the contribution between \mathcal{L}_{FKL} and \mathcal{L}_{RKL} .

Figure 5 shows that average accuracy scores are higher when $\lambda_{\text{KL}} = 0.1$. Although the highest accuracy is achieved with $\lambda_{\text{KL}} = 0.1$, $\alpha = 0.5$, and $\tau = 1.0$, the gap remains larger than in the setting with $\lambda_{\text{KL}} = 0.1$, $\alpha = 0.2$, and $\tau = 1.0$. To balance maximizing accuracy and minimizing the gap, we ultimately select the combination $\lambda_{\text{KL}} = 0.1$, $\alpha = 0.2$, and $\tau = 1.0$.

Detailed Experiment Results

Our primary evaluation was conducted on three benchmarks: MATHVERSE, MATHVISTA, and WE-MATH. The experimental results are discussed in detail below.

Performance on MATHVERSE

The distinguishing feature of MATHVERSE is its capacity to evaluate the model’s performance on identical information problems under varying degrees of multimodal richness. Consequently, an examination of the discrepancy between each category represents an intriguing and valuable undertaking. Before the discussion, let us briefly introduce the six evaluation categories of MATHVERSE:

- **Text-dominant:** The most prevalent single-image format for text-based inquiries is one in which the entirety of the original question’s textual content is retained. In most cases, the image serves as an additional clarification to the text; however, it may occasionally contain essential information.
- **Text-lite:** Redundant information is removed from the original question, ensuring that only essential information remains in the text, avoiding any repetition of information conveyed by both text and image. This category assesses the model’s multimodal capabilities, as the absence of effective information extraction from the image would render the question incomplete.

- **Vision-intensive:** In comparison to text-lite, this category represents a further reduction in implicit attributes within the text. However, it is acknowledged that the transfer of information is not always complete, and vision-intensive questions may sometimes confuse humans as well.
- **Vision-dominant:** This category is not merely an enhancement of vision-intensive in terms of visual information but rather compared to text-lite, it annotates necessary textual information within the image, such as angle measurements, lengths of sides, etc.
- **Vision-only:** This category retains only the image, transferring all text to the image. Thus, it assesses not only the model’s image recognition capability but also its OCR capability, as the question still appears in text format within the image.
- ***Text-only:** This category needs to be mentioned separately as it is not a purely textual version equivalent to the original question. Unlike the text-only concept mentioned in our main text, it merely removes the image from the text-dominant version, sometimes lacking some information such as the basic shape of functions, etc. According to MATHVERSE, this category helps determine whether MLLMs primarily rely on descriptive information or contextual visual information from diagrams to solve problems. We provide it here for reference.

As shown in Table 5, our model leads across multiple metrics, surpassing all similarly scaled open-source models and some closed-source models, approaching the performance of the best model, GPT-4V. Additionally, it is evident that the performance gap between vision-based and text-based questions for our model is smaller compared to GPT-4V. However, we also acknowledge that there is still a significant gap between our model’s performance and that of humans. Future efforts should focus on bridging this gap and aligning modalities.

Table 6 presents more detailed scores for subcategories within three main categories reported by MATHVERSE: Plane Geometry, Solid Geometry, and Functions. Each category reports both the total score and the scores for their respective subcategories. It can be observed that our model has a good understanding of planar-type questions, with very optimistic scores in Plane Geometry and Functions. In contrast, the scores for Solid Geometry are relatively average. This trend is also reflected in other open-source models, indicating that current MLLMs have weaker perceptual abilities in solid geometry. This represents a potential direction for future research advancements.

Performance on MATHVISTA

MATHVISTA is a comprehensive visual environment reasoning benchmark. It is not limited to traditional exam-style questions but includes a broader range of visual reasoning scenarios such as charts, real-world photographs, and external knowledge inference. Its sources are diverse, including traditional datasets like AI2D and Geometry3K, as well as newly created ones such as IQTest and PaperQA. It encom-

Table 5: **Mathematical evaluation on MATHVERSE *testmini* set.** We calculate the “ALL” score without averaging the “Text-only” version. For closed-source and open-source MLLMs, the best accuracy scores are marked in **bold** fonts, while the second best accuracy scores are marked in underline fonts, respectively.

Model	# Params.	MATHVERSE						
		ALL	Text-dom.	Text-lite	Text-only	Vision-int.	Vision-dom.	Vision-only
<i>Baselines</i>								
Random chance	-	12.4	12.4	12.4	12.4	12.4	12.4	12.4
Human performance	-	64.9	71.2	70.9	41.7	61.4	68.3	66.7
<i>Closed-source LLMs</i>								
ChatGPT (Ouyang et al. 2022)	-	-	33.3	18.9	33.3	-	-	-
GPT-4 (OpenAI 2023a)	-	-	46.5	20.7	46.5	-	-	-
<i>Closed-source MLLMs</i>								
Qwen-VL-Plus (Bai et al. 2023)	-	11.8	15.7	11.1	14.5	9.0	13.0	10.0
Gemini-1.0-Pro (Gemini Team 2023)	-	22.3	27.6	23.7	27.9	19.4	20.3	20.5
Qwen-VL-Max (Bai et al. 2023)	-	24.8	30.3	24.8	32.2	20.6	23.3	25.1
GPT-4V (OpenAI 2023b)	-	38.3	52.1	40.9	46.1	34.9	33.6	29.8
<i>Open-source MLLMs</i>								
mPLUG-Owl2 (Ye et al. 2024)	7B	4.6	6.6	6.3	6.1	6.3	5.6	4.9
LLaMA-Adapter-V2 (Gao et al. 2023b)	7B	5.7	6.2	5.9	2.7	6.1	4.2	6.1
LLaVA-1.5 (Liu et al. 2024a)	13B	7.6	8.8	7.6	11.5	7.4	7.4	6.9
LLaVA-NeXT (Liu et al. 2024b)	8B	10.3	12.8	12.0	9.9	10.7	9.7	6.3
MiniGPT-v2 (Chen et al. 2023a)	7B	11.0	12.1	12.0	11.7	13.1	10.3	7.4
SPHINX-Plus (Gao et al. 2024)	13B	12.2	13.9	11.6	14.9	11.6	13.5	10.4
ShareGPT4V (Chen et al. 2023b)	13B	13.1	16.2	6.6	16.2	15.5	13.8	3.7
InternLM-XC2. (Dong et al. 2024)	7B	16.3	20.2	14.3	24.5	14.2	17.5	15.2
G-LLaVA (Gao et al. 2023a)	7B	16.6	20.9	20.7	21.1	17.2	14.6	9.4
SPHINX-MoE (Gao et al. 2024)	8×7B	16.8	26.2	17.4	26.7	16.7	12.5	11.1
DeepSeek-VL (Lu et al. 2024a)	7B	19.3	23.0	23.2	23.1	20.2	18.4	11.8
Math-LLaVA (Shi et al. 2024)	13B	22.9	27.3	24.9	27.0	24.5	21.7	16.1
Math-PUMA-Qwen2-1.5B	1.5B	29.6	35.8	32.2	35.2	31.3	<u>30.4</u>	<u>18.5</u>
Math-PUMA-Qwen2-7B	7B	33.6	<u>42.1</u>	<u>35.0</u>	<u>39.8</u>	<u>33.4</u>	31.6	26.0
Math-PUMA-DeepSeek-Math-7B	7B	<u>31.8</u>	43.4	35.4	47.5	33.6	31.6	14.7

Table 6: **Mathematical Evaluation on different subjects and subfields in MATHVERSE *testmini* set.** ‘TO’ indicates that the scores are averaged over five problem versions of the ‘Text-only’ version. Without TO, the scores are averaged over five problem versions, excluding the ‘Text-only’ version. Len: Length; Anal: Analytic; Apply: Applied; Vol: Volume; Coord: Coordinate; Prop: Property; Exp: Expression; Apply: Applied. The best accuracy scores without TO are marked in **bold** fonts.

Model	# Params.	Plane Geometry						Solid Geometry				Functions				
		All	Len	Area	Angle	Anal	Apply	All	Len	Area	Vol	All	Coord	Prop	Exp	Apply
LLaVA-1.5	7B	15.9	15.7	14.5	18.8	7.0	14.8	2.7	4.2	1.8	2.7	20.9	7.5	26.8	8.1	26.0
LLaVA-1.5 (TO)	7B	16.3	15.2	17.0	15.5	16.3	20.3	5.9	4.2	0.0	11.8	20.1	18.8	21.1	6.2	30.0
Math-LLaVA	13B	27.6	28.1	29.8	31.6	7.9	26.4	3.5	7.5	1.8	3.1	22.1	8.7	22.3	8.1	38.5
Math-LLaVA (TO)	13B	33.5	32.9	38.3	37.3	14.0	33.3	5.9	12.5	2.3	5.9	22.0	31.2	19.7	3.1	37.5
Math-PUMA-Qwen2-7B	7B	37.1	41.1	37.0	37.9	32.6	28.1	17.5	23.3	7.7	23.1	34.7	43.8	39.4	13.8	39.5
Math-PUMA-Qwen2-7B (TO)	7B	43.7	46.2	38.3	45.1	39.5	40.6	35.8	45.8	18.2	29.4	35.8	43.8	43.7	25.0	27.5
Math-PUMA-DeepSeek-Math-7B	7B	37.8	38.7	36.6	45.0	23.3	25.8	9.2	12.5	5.5	11.0	29.1	28.7	29.0	16.9	39.0
Math-PUMA-DeepSeek-Math-7B (TO)	7B	50.2	53.2	44.7	54.9	44.2	37.7	39.4	37.5	18.2	35.3	52.2	62.5	52.1	59.4	42.5

passes both real and synthetic scenes and supports multiple languages, including Chinese and English.

We will now focus more on the scores of each subcategory to explore the model’s capabilities in different directions in detail.

Task & Skills In this section we focus on analysing the tasks and skills of the model and the results are displayed in

Table 7.

- **Advantages:** Due to our model being trained on higher-quality mathematical reasoning data, it demonstrates strong competitiveness in some rigorously formatted exam-style questions, such as:

- GPS (Geometry Problem Solving): Our most advanced model achieved an accuracy of 48.1%, nearly

Table 7: **Mathematical evaluation on MATHVISTA *testmini* set.** Task types: FQA: figure QA, GPS: geometry problem solving, MWP: math word problem, TQA: textbook QA, VQA: visual QA. Math reasoning types: ALG: algebraic, ARI: arithmetic, GEO: geometry, LOG: logical, NUM: numeric, SCI: scientific, STA: statistical. For closed-source and open-source MLLMs, the best accuracy scores are marked in **bold** fonts, while the second best accuracy scores are marked in underline fonts, respectively.

Model	# Params.	ALL	FQA	GPS	MWP	TQA	VQA	ALG	ARI	GEO	LOG	NUM	SCI	STA
<i>Baselines</i>														
Random chance	-	17.9	15.5	24.1	4.5	23.4	24.3	25.8	13.8	22.7	13.4	8.8	15.8	14.3
Human performance	-	60.3	59.7	48.4	73.0	63.2	55.9	50.9	59.2	51.4	40.7	53.8	64.9	63.9
<i>Closed-source LLMs</i>														
ChatGPT (Ouyang et al. 2022)	-	33.2	26.0	31.7	35.5	48.1	30.2	32.4	32.3	33.0	16.2	17.4	54.9	36.2
GPT-4 (OpenAI 2023a)	-	33.2	27.9	31.7	31.2	51.9	28.5	33.5	30.9	32.2	13.5	12.5	58.2	37.9
<i>Closed-source MLLMs</i>														
Qwen-VL-Plus (Bai et al. 2023)	-	43.3	54.6	38.5	31.2	55.1	34.1	39.1	32.0	39.3	18.9	26.4	59.0	56.1
Gemini-1.0-Pro (Gemini Team 2023)	-	45.2	47.6	40.4	39.2	61.4	39.1	45.2	38.8	41.0	10.8	32.6	54.9	56.8
GPT-4V (OpenAI 2023b)	-	49.9	43.1	50.5	57.5	65.2	38.0	53.0	49.0	51.0	21.6	20.1	63.1	55.8
<i>Open-source MLLMs</i>														
mPLUG-Owl2 (Ye et al. 2024)	7B	22.2	22.7	23.6	10.2	27.2	27.9	23.6	19.2	23.9	13.5	12.7	26.3	21.4
LLaMA-Adapter-V2 (Gao et al. 2023b)	7B	23.9	21.2	25.5	11.3	32.3	31.8	26.3	20.4	24.3	24.3	13.9	29.5	18.3
LLaVA-1.5 (Liu et al. 2024a)	13B	25.7	23.1	18.3	22.0	29.1	<u>39.1</u>	19.6	28.6	17.6	10.8	27.8	33.6	22.9
MiniGPT-v2 (Chen et al. 2023a)	7B	23.1	18.6	26.0	13.4	30.4	30.2	28.1	21.0	24.7	16.2	16.7	25.4	17.9
InternLM-XC2. (Dong et al. 2024)	7B	47.8	53.2	31.7	76.3	39.2	36.3	32.0	51.6	30.5	13.5	43.8	37.7	62.8
G-LLaVA (Gao et al. 2023a)	7B	23.8	16.0	38.9	14.0	24.1	27.9	36.3	18.4	35.6	16.2	18.1	20.5	14.6
SPHINX-MoE (Gao et al. 2024)	8×7B	42.3	<u>49.8</u>	31.2	42.5	46.8	39.7	31.7	41.6	30.5	16.2	27.1	50.8	50.8
DeepSeek-VL (Lu et al. 2024a)	7B	34.9	<u>26.8</u>	28.4	55.9	32.9	34.6	29.2	38.8	27.2	18.9	<u>43.1</u>	35.3	33.2
Math-LLaVA (Shi et al. 2024)	13B	38.3	37.2	29.3	55.9	36.7	33.5	28.5	39.1	30.5	18.9	36.8	42.6	42.2
Math-PUMA-Qwen2-1.5B	1.5B	44.5	38.3	<u>47.6</u>	<u>70.4</u>	37.3	29.6	<u>43.4</u>	43.9	47.3	16.2	34.0	41.0	47.5
Math-PUMA-Qwen2-7B	7B	47.9	46.5	48.1	<u>68.3</u>	46.2	30.2	47.7	<u>46.2</u>	47.3	<u>21.6</u>	32.6	42.6	<u>55.8</u>
Math-PUMA-DeepSeek-Math-7B	7B	44.7	42.8	39.9	67.7	42.4	31.3	39.2	41.9	<u>41.4</u>	8.1	36.8	<u>48.4</u>	52.5

Table 8: **Accuracy scores on MATHVISTA *testmini* set.** Abs. scene: Abstract scene; Doc. image: Document image; Func. plot: Function plot; Geo. diagram: Geometry diagram; Med. image: Medical image; Sci. figure: Scientific figure; Syn. scene: Synthetic scene. The best accuracy scores are marked in **bold** fonts.

Model	# Params.	Abs. scene	Bar chart	Doc. image	Func. plot	Geo. diagram	Line plot	Map chart	Med. image	Natural image	Pie chart	Puzzle test	Scatter plot	Sci. figure	Syn. scene	Table
LLaVA-1.5 (Liu et al. 2024a)	7B	24.59	18.49	16.67	33.87	22.22	30.77	62.50	33.33	22.94	33.33	16.67	27.78	29.35	32.26	18.57
LLaVA-1.5 (Liu et al. 2024a)	13B	24.59	21.85	16.67	25.81	18.52	30.77	50.00	66.70	30.28	41.67	11.11	25.00	30.43	29.52	15.71
InternLM-XC2. (Dong et al. 2024)	7B	78.69	73.11	41.67	37.10	30.56	43.59	62.50	33.33	29.36	66.67	13.89	50.00	39.13	62.90	70.00
G-LLaVA (Gao et al. 2023a)	13B	27.87	10.08	0.00	33.87	37.96	38.46	37.50	100.00	13.76	16.67	16.67	16.67	17.39	28.23	7.14
DeepSeek-VL (Lu et al. 2024a)	7B	81.97	22.69	16.67	37.10	27.78	41.03	62.50	33.30	26.61	41.67	19.44	25.00	28.26	43.55	50.00
Math-LLaVA (Shi et al. 2024)	13B	55.74	42.86	16.67	30.65	31.94	43.59	62.50	33.33	22.94	41.67	19.44	33.33	41.30	50.81	48.57
Math-PUMA-Qwen2-1.5B	1.5B	72.13	42.02	16.67	37.10	48.61	53.85	37.50	100.00	15.60	58.33	16.67	38.89	36.96	56.45	64.29
Math-PUMA-Qwen2-7B	7B	65.57	54.62	33.33	56.45	50.00	51.28	62.50	33.00	16.51	58.33	19.44	44.44	39.13	54.03	70.00
Math-PUMA-DeepSeek-Math-7B	7B	72.13	42.02	16.67	37.10	48.61	53.85	37.50	100.00	15.60	58.33	16.67	38.89	36.96	56.45	64.29

matching the human performance of 48.4%.

- MWP (Math World Problem): Our three models achieved high performance, scoring 70.4%, 68.3%, and 67.7%, respectively, closely approaching the human performance of 73.0%.
- ALG (Algebraic): Our models secured the top-2 positions among the open-source models reported, with the most advanced model achieving an accuracy of 47.7%, very close to the human performance of 50.9%.
- GEO (Geometry): Our models also secured the top-2 positions among the open-source models reported, with the most advanced model achieving an accuracy of 47.3%, not far from the human performance of

51.4%.

These results indicate that our model exhibits excellent mathematical reasoning capabilities, leading among open-source models and closely approximating human performance, which fully demonstrates the effectiveness of our approach in mathematical reasoning.

- **Disadvantages:** However, our model also shows room for improvement in some areas, such as:

- FQA (Figure QA): Our most advanced model has achieved 46.5%, which is comparable to GPT-4V’s 43.1% and Gemini-1.0-Pro’s 47.6%, but still falls short of the human performance of 59.7%.

Table 9: **Evaluation results on MATHVISTA *testmini* set.** The best scores of each category are marked in **bold** fonts.

Model	# Params.	Question Type			Grade				Language		Category	
		Free Form	Multi Choice	Elementary School	High School	College	Not Applicable	Chinese	English	General-VQA	Math-Targeted-VQA	
LLaVA-1.5 (Liu et al. 2024a)	7B	9.13	38.89	15.92	27.12	25.89	28.35	29.03	25.00	30.87	20.37	
LLaVA-1.5 (Liu et al. 2024a)	13B	14.35	35.37	21.39	24.18	20.54	30.71	20.97	26.07	33.26	19.26	
InternLM-XC2. (Dong et al. 2024)	7B	50.22	45.74	63.68	42.16	22.32	51.44	40.32	48.40	52.39	43.89	
G-LLaVA (Gao et al. 2023a)	7B	5.43	39.44	15.92	33.01	23.21	20.73	51.61	22.01	22.17	25.19	
DeepSeek-VL (Lu et al. 2024a)	7B	27.61	41.11	51.74	32.68	28.57	29.66	32.26	35.04	32.17	37.22	
Math-LLaVA (Shi et al. 2024)	13B	30.65	44.81	48.26	38.89	24.11	36.75	27.42	39.10	40.22	36.67	
Math-PUMA-Qwen2-1.5B	1.5B	36.74	51.11	59.20	50.98	30.36	35.70	48.39	44.34	38.70	49.44	
Math-PUMA-Qwen2-7B	7B	42.83	52.22	57.71	52.29	41.07	41.21	56.45	47.44	43.26	51.85	
Math-PUMA-DeepSeek-Math-7B	7B	36.52	51.67	57.21	47.39	33.93	39.11	40.32	45.09	43.48	45.74	

Table 10: **Accuracy scores on WE-MATH *testmini* set.** S1: one-step problem, S2: two-step problem, S3: three-step problem, Mem: Measurement, PF: Plane Figures, SF: Solid Figures, TMF: Transformations and Motion of Figures, PD: Position and Direction. AL: Angles and Length, UCU: Understanding and Conversion of Units, CPF: Calculation of Plane Figures, UPF: Understanding of Plane Figures, CSF: Calculation of Solid Figures, USF: Understanding of Solid Figures, BTF: Basic Transformations of Figures, CCF: Cutting and Combining of Figures, Dir: Direction, Pos: Position, RoM: Route Map, CCP: Correspondence of Coordinates and Positions. For open-source MLLMs ($\approx 10B$), the best scores of each category are marked in **bold** fonts.

Model	# Params.	S1	S2	S3	Mem		PF		SF		TMF		PD			
					UCU	AL	CPF	UPF	CSF	USF	BTF	CCF	Dir	Pos	RoM	CCP
<i>Closed-source MLLMs</i>																
Qwen-VL-Max (Bai et al. 2023)	-	40.8	30.3	20.6	19.4	25.3	39.8	41.4	43.6	48.0	43.8	26.7	41.4	35.1	40.7	26.7
Gemini-1.5-Pro (Reid et al. 2024)	-	56.1	51.4	33.9	51.0	31.2	61.8	45.0	70.0	57.5	39.2	60.0	68.8	54.1	40.7	60.0
GPT-4V (OpenAI 2023b)	-	65.5	49.2	38.2	82.5	38.4	70.7	60.2	76.6	56.3	57.8	63.3	79.3	57.5	47.8	63.3
GPT-4o (OpenAI 2024b)	-	73.3	57.2	46.1	87.1	45.8	76.7	71.0	82.2	65.7	58.1	70.0	93.1	80.4	58.8	70.0
<i>Open-source MLLMs ($\geq 20B$)</i>																
InternVL-Chat-V1.5 (Chen et al. 2024)	26B	49.4	30.6	28.5	44.0	29.8	52.2	52.1	44.2	48.2	47.1	36.7	65.7	50.5	36.5	36.7
LLaVA-NeXT (Liu et al. 2024b)	72B	42.9	35.6	30.9	31.7	25.3	43.3	42.4	46.1	41.8	44.2	36.7	44.3	39.0	33.0	36.7
LLaVA-NeXT (Liu et al. 2024b)	110B	53.7	36.9	31.5	39.5	57.7	59.5	53.1	52.3	50.2	54.1	40.0	54.8	55.9	40.1	40.0
<i>Open-source MLLMs ($\approx 10B$)</i>																
LLaVA-1.5 (Liu et al. 2024a)	7B	30.5	29.7	29.7	33.7	28.4	20.0	38.9	28.6	35.6	40.4	32.2	20.7	21.2	51.7	43.3
LLaVA-1.5 (Liu et al. 2024a)	13B	35.4	30.0	32.7	27.1	49.0	25.3	44.1	31.4	35.7	48.5	38.9	43.8	37.7	36.5	36.7
LLaVA-1.6 (Liu et al. 2024b)	7B	23.0	20.8	15.8	18.5	20.5	16.9	29.6	15.6	18.6	42.7	26.7	17.6	43.3	28.9	26.7
LLaVA-1.6 (Liu et al. 2024b)	13B	29.4	25.3	32.7	21.7	23.2	23.4	34.7	25.3	26.4	37.5	30.0	26.9	28.9	37.1	30.0
DeepSeek-VL (Lu et al. 2024a)	7B	32.6	26.7	25.5	16.6	35.1	27.3	38.0	24.2	38.7	50.0	23.3	24.5	41.0	51.7	23.3
G-LLaVA (Gao et al. 2023a)	13B	32.4	30.6	32.7	33.3	29.1	32.0	37.9	19.6	33.5	37.1	40.0	31.2	33.2	25.6	40.0
Math-LLaVA (Shi et al. 2024)	13B	38.7	34.2	34.6	30.3	17.9	39.2	40.4	37.1	37.7	53.0	51.3	30.8	30.8	40.9	46.7
InternLM-XC2. (Dong et al. 2024)	7B	47.0	33.1	33.3	31.3	46.5	47.7	42.6	51.4	43.9	41.1	40.0	65.5	53.9	55.2	40.0
Math-PUMA-Qwen2-1.5B	1.5B	37.0	31.7	27.3	25.5	27.9	37.9	32.5	41.3	42.7	36.4	50.1	27.6	31.5	18.4	46.7
Math-PUMA-Qwen2-7B	7B	53.3	39.4	36.4	63.5	42.5	60.2	45.9	66.2	48.6	42.3	53.5	31.2	37.7	40.4	46.7
Math-PUMA-DeepSeek-Math-7B	7B	45.6	38.1	33.9	69.8	29.1	45.7	38.6	51.8	43.6	41.6	54.6	44.8	53.8	29.1	40.0

- LOG (Logical): Our most advanced model has reached an accuracy of 21.6%, surpassing Qwen-VL-Plus and Gemini-1.0-Pro, and being on par with GPT-4V. However, it still has a significant gap compared to the human performance of 40.7%.
- NUM (Numeric): Our models scored 34.0%, 32.6%, and 36.8%, respectively, outperforming the best closed-source model GPT-4V’s 21.6%, but still exhibiting a considerable gap from the human performance of 53.8%.

Our objective is to further align and approach human-level performance, and thus, these areas remain a focal

point for improvement.

Context In Table 8, we present the performance of our model under different contexts. Consistent with the analysis earlier, our model shows outstanding performance in geometry-related tasks. For example, our model significantly outperforms others in function plots, geometry diagrams, and line plots. For standard visual question answering tasks, such as bar charts, map charts, and pie charts, our model also performs well. However, our model underperforms in scenarios involving natural images. Our preliminary conclusion is that this is due to the limited training data for this category, which is a potential direction for future im-

Table 11: **Evaluation results on WE-MATH *testmini* set.** AVG: average score, IK: Insufficient Knowledge, IG: Inadequate Generalization, CM: Complete Mastery, RM: Rote Memorization. The best scores of each category are marked in **bold** fonts.

Model	# Params.	Strict					Loose				
		Avg \uparrow	IK \downarrow	IG \uparrow	CM \uparrow	RM \downarrow	Avg \uparrow	IK \downarrow	IG \uparrow	CM \uparrow	RM \downarrow
<i>Closed-source MLLMs</i>											
Qwen-VL-Max (Bai et al. 2023)	-	10.5	65.1	7.6	6.7	75.5	25.5	65.1	7.6	21.7	20.3
Gemini-1.5-Pro (Reid et al. 2024)	-	26.4	42.9	11.2	20.8	54.8	46.0	42.9	11.2	40.4	12.0
GPT-4V (OpenAI 2023b)	-	31.1	39.8	14.5	23.8	47.9	51.4	39.8	14.5	44.2	3.3
GPT-4o (OpenAI 2024b)	-	42.9	31.2	15.2	35.2	34.2	60.6	31.2	15.2	53.0	1.1
<i>Open-source MLLMs ($\geq 20B$)</i>											
InternVL-Chat-V1.5 (Chen et al. 2024)	26B	12.7	56.4	10.5	7.4	77.6	31.0	56.4	10.5	25.7	22.4
LLaVA-NeXT (Liu et al. 2024b)	72B	13.4	58.9	7.1	9.9	71.0	31.5	58.9	7.1	28.0	17.9
LLaVA-NeXT (Liu et al. 2024b)	110B	19.2	50.3	14.5	12.0	66.0	37.9	50.3	14.5	30.7	13.0
<i>Open-source MLLMs ($\approx 10B$)</i>											
LLaVA-1.5 (Liu et al. 2024a)	7B	6.8	65.1	5.1	4.2	85.9	24.1	65.1	5.1	21.5	27.6
LLaVA-1.5 (Liu et al. 2024a)	13B	9.3	65.0	4.2	7.2	76.5	24.4	65.0	4.2	22.3	27.8
LLaVA-1.6 (Liu et al. 2024b)	7B	3.3	78.3	2.5	2.1	89.1	13.8	78.3	2.5	12.6	34.7
LLaVA-1.6 (Liu et al. 2024b)	13B	5.2	69.1	3.2	3.6	86.9	22.0	69.1	3.2	20.4	26.2
DeepSeek-VL (Lu et al. 2024a)	7B	6.3	69.1	4.6	4.0	84.8	21.0	69.1	4.6	18.7	29.0
Math-LLaVA (Shi et al. 2024)	13B	11.1	62.1	3.6	9.3	72.8	31.3	62.1	3.6	29.5	13.9
InternLM-XC2. (Dong et al. 2024)	7B	12.7	56.4	10.5	7.4	77.6	31.0	56.4	10.5	25.7	22.4
Math-PUMA-Qwen2-1.5B	1.5B	10.4	63.8	5.9	7.4	75.5	26.4	63.8	5.9	23.4	22.6
Math-PUMA-Qwen2-7B	7B	19.2	47.8	13.7	12.4	67.8	41.0	47.8	13.7	34.1	11.4
Math-PUMA-DeepSeek-Math-7B	7B	15.6	56.0	7.2	12.0	67.4	35.8	56.0	7.2	32.2	12.4

provement.

Others In Table 9, we also present the scores for other categories in MATHVISTA. Several interesting observations can be noted:

- Our model performs well in both free-form and multiple-choice question types, indicating that the model is not only capable of selecting options but also has some dialogue and continuation abilities. We also noticed that while all open-source models perform well on multiple-choice questions, some models show significantly lower scores in free-form questions. This may be due to the training data overly focusing on common multiple-choice questions.
- Our model excels in more challenging questions at the high school level and above. It can be observed that open-source models generally perform well on elementary school-level questions but struggle with higher difficulty questions at the high school and college levels. Our model, however, performs exceptionally well on these challenging questions, demonstrating its deeper reasoning capabilities.
- Our model shows balanced performance in both Chinese and English language questions. It is noticeable that some open-source models may prefer to solve questions in a single language. We speculate that this could be due to the base LLM’s limitations, such as LLaVA models commonly being trained on English corpora, or the SFT data having biases, such as certain language data and questions being easier to collect.

Performance on WE-MATH

WE-MATH is a benchmark that emphasizes mathematical reasoning, making it highly relevant to our research focus. Unlike existing benchmarks, it is constructed around textbook knowledge units, decomposing problem-solving into subproblems based on knowledge concepts.

Accuracy As shown in Table 10, WE-MATH evaluates scores for S1 (one-step), S2 (two-step), and S3 (three-step) problems, as well as multiple categories of questions.

In S1, S2, and S3, our models performed exceptionally well. Our best model not only achieved state-of-the-art results among models of similar scale but also demonstrated comparable performance to significantly larger models. Specifically, our model scored 53.3, 39.4, and 36.4 for the three steps, respectively, which are comparable to LLaVA-NeXT-110B’s 53.7, 36.9, and 31.5. This indicates that our model possesses reasoning abilities comparable to large-scale MLLMs, substantiating the effectiveness of our approach.

In other categories, consistent with the findings in MATHVISTA, our model excels in geometric reasoning. For example, in CPF (Calculation of Plane Figures), UPF (Understanding of Plane Figures), CSF (Calculation of Solid Figures), and USF (Understanding of Solid Figures), our best model achieved the best performance among open-source models of similar scale and performed comparably to larger open-source MLLMs. Our model also demonstrated complex understanding capabilities, achieving state-of-the-art performance among models of similar scale in CCF (Cutting and Combining of Figures) and CCP (Correspondence

of Coordinates and Positions).

Four Dimensional Metrics WE-MATH provides four dimensions of evaluation metrics: IK (Insufficient Knowledge), IG (Inadequate Generalization), CM (Complete Mastery), and RM (Rote Memorization). We briefly introduce each metric for subsequent analysis:

- **Insufficient Knowledge (IK):** Part of one-step problems contain errors, and the multi-step problem is wrong. This is reasonable because the model’s insufficient grasp of single knowledge concepts may lead to errors in multi-step problems.
- **Inadequate Generalization (IG):** One-step problems are all correct, but the multi-step problem is incorrect. This is also considered reasonable. While LMMs are capable of understanding individual knowledge concepts, they may struggle to generalize that knowledge to solve composite problems.
- **Complete Mastery (CM):** One-step problems are all correct, and the multi-step problem is also answered correctly. This result demonstrates that the model’s results are both reliable and accurate.
- **Rote Memorization (RM):** One-step problems contain errors, but the multi-step problem is answered correctly, which contradicts human logical thinking. If a model can solve composite multi-step problems but fails to answer the one-step problems needed in the process, it raises doubts about the model’s reliability.

As shown in Table 11, our model not only demonstrates competitiveness in the average score but also matches the performance of large-scale MLLMs like LLaVA-NeXT-110B in IK and RM metrics, and outperforms closed-source models like Qwen-VL-Max. This indicates that our model does not merely memorize or recite questions but has begun to exhibit intrinsic reasoning capabilities, showing good generalization performance and the ability to solve extended problems.

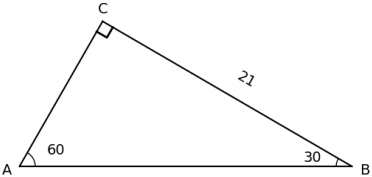
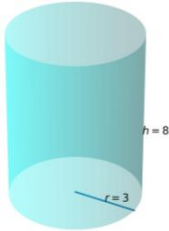
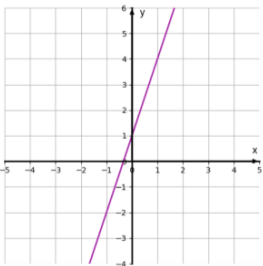
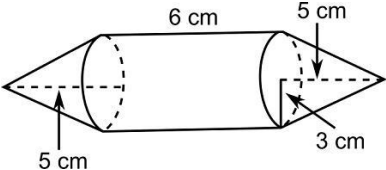
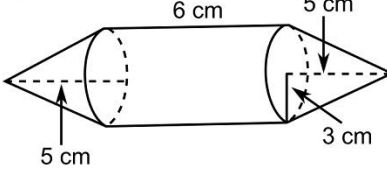
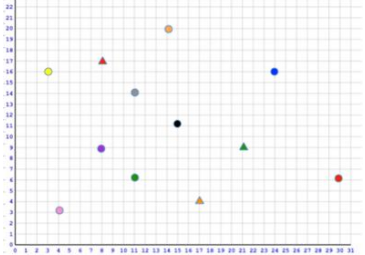
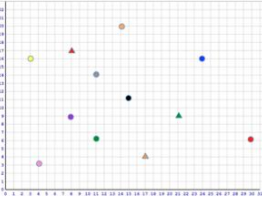
Text-rich	Vision-rich	Solution
<p>In triangle ABC, if assuming angle $A=60^\circ$, and angle $B=30^\circ$, with $BC=21$, what's AB?</p>	<p>Compute AB.</p> 	<p>Given the conditions, we can find the length of AB using trigonometric relationships. First, ... Final answer: $14\sqrt{3}$</p>
<p>The height of a cylinder is 8, and the radius of the cylinder is 3, calculate the surface area of the cylinder.</p>	<p>Calculate the surface area of the cylinder.</p> 	<p>To calculate the surface area of a cylinder, we need to ... So, the surface area of the cylinder is: 66π</p>
<p>Identify the equation of the function $y = a * x + b$ passing through points $(1,4)(0,1)$.</p>	<p>Identify the equation.</p> 	<p>To identify the equation of the function ... Therefore, the equation of the function is: $y = 3x + 1$</p>
<p>Calculate the surface area of the cylindrical part of the figure.</p> 	<p>Calculate the surface area of the cylindrical part of the figure.</p> 	<p>The surface area of the cylindrical part of the figure includes the lateral surface area since the bases are not exposed ... we get: Lateral surface area = $2 \times \pi \times 3 \times 6 = 36\pi \text{ cm}^2$</p>
<p>Calculate the surface area of the cylindrical part of the figure.</p> 	<p>What coordinate point is the red circle on? Possible Answers: (6,30) (8,17) (30,6) (17,8)</p> 	<p>The red circle is positioned at the coordinate point $(30,6)$, indicating that it lies at 30 on the x-axis and 6 on the y-axis.</p>

Figure 6: Examples of training dataset at stage 2.

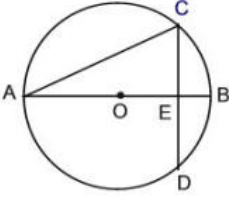
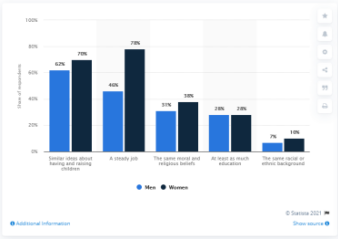

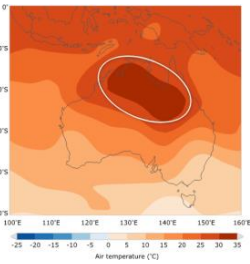
Question Type and Image	Question	Solution								
<p><i>Geometry Problem Solving</i></p> 	<p><i>In circle O, diameter AB is perpendicular to chord CD at E. If $CD = 8$ and $BE = 2$, find AE. Choices: (A) $2\sqrt{5}$ (B) 8 (C) 10 (D) 16</i></p>	<p><i>To determine the length of AE, we can employ various properties of circles and the Pythagorean theorem. Firstly, ... Answer: B. 8</i></p>								
<p><i>Math Word Problem</i></p> <table border="1" data-bbox="191 611 537 751"> <tr> <td>pineapple upside-down cake</td> <td>\$8.29</td> </tr> <tr> <td>banana cream pie</td> <td>\$9.79</td> </tr> <tr> <td>chocolate cheesecake</td> <td>\$8.22</td> </tr> <tr> <td>peach pie</td> <td>\$8.35</td> </tr> </table>	pineapple upside-down cake	\$8.29	banana cream pie	\$9.79	chocolate cheesecake	\$8.22	peach pie	\$8.35	<p><i>Vincent has \$16.71. Does he have enough to buy a pineapple upside-down cake and a peach pie? Choices: (A) yes (B) no</i></p>	<p><i>Vincent has \$16.71. Let's see if he has enough money to buy a pineapple upside-down cake and a peach pie ... Therefore, the answer is (A) yes.</i></p>
pineapple upside-down cake	\$8.29									
banana cream pie	\$9.79									
chocolate cheesecake	\$8.22									
peach pie	\$8.35									
<p><i>Figure Question Answering</i></p> 	<p><i>What is the average percentage of respondents for men across all categories?</i></p>	<p><i>The data includes five categories: "Similar ideas about having children", "A steady job", ... Overall, the average percentage of respondents for men across all categories is 34.8%.</i></p>								
<p><i>Visual Question Answering</i></p> 	<p><i>What sort of building is seen behind this amusement? Choices: (A) school (B) barn (C) cafe (D) financial</i></p>	<p><i>The image shows a modern building with large windows in the background. The text "UBS" is visible on ... Therefore, the correct answer is (D) financial.</i></p>								
<p><i>Textbook Question Answering</i></p> 	<p><i>What is the approximate latitude range of the outlined area shown?</i></p>	<p><i>The image shows an air temperature map of Australia with the area of concern outlined in white. The air ... Answer: 10°S to 30°S</i></p>								

Figure 7: Examples of training dataset at stage 3.